NASA CONTRACTOR REPORT

NASA CR-1692

HEAT TRANSFER ON A FLAT PLATE IN CONTINUUM TO RAREFIED HYPERSONIC FLOWS AT MACH NUMBERS OF 19.2 AND 25.4

by H. T. Nagamatsu, W. T. Pettit, and R. E. Sheer, Jr.

Prepared by
GENERAL ELECTRIC RESEARCH AND DEVELOPMENT CENTER
Schenectady, N. Y.
for

NATIONAL AERONAUTICS AND SPACE ADMINISTRATION • WASHINGTON, D. C. • NOVEMBER 1970

1. Report No.	2. Government Accession No.	3. Recipient's Catalog No.
NASA CR-1692		

4. Title and Subtitle	5. Report Date
HEAT TRANSFER ON A FLAT PLATE IN CONTINUUM TO RAREFIED HYPERSONIC FLOWS AT MACH NUMBERS OF 19.2 AND 25.4	November 1970
	6. Performing Organization Code
7. Author(s) H. T. Nagamatsu, W. T. Pettit, and R. E. Sheer, Jr.	8. Performing Organization Report No.
9. Performing Organization Name and Address General Electric Research and Development Center Schenectady, New York	10. Work Unit No.
	11. Contract or Grant No. NASW-1785
	13. Type of Report and Period Covered Contractor Report
12. Sponsoring Agency Name and Address National Aeronautics and Space Administration Washington, D. C. 20546	14. Sponsoring Agency Code

15. Supplementary Notes

16. Abstract

Surface heat transfer rates were measured on a sharp flat plate at zero angle of attack in a hypersonic shock tunnel at flow Mach numbers of 19.2 and 25.4. The density and Knudsen number were altered to span the continuum to near free molecule flow regimes. For both Mach numbers, the heat transfer data agree reasonably well with the strong interaction predictions of Li and Nagamatsu for Reynolds number per inch greater than 10^4 and leading edge Knudsen numbers less than 4. Below a unit Reynolds number of 10^4 a systematic reduction in the heat transfer rate close to the leading edge was observed for both Mach numbers. Furthermore, the Stanton number remained relatively constant independent of Mach number and unit Reynolds number.

17. Key Words (Selected by Author(s))	18. Distribution Statement
Surface heat transfer flat plate hypersonic continuum free molecule flow 1. Heat Transfer 2. Hypersonic Flow	Unclassified - Unlimited

19. Security Classif. (of this report)	20. Security Classif. (of this page)	21. No. of Pages	22. Price
Unclassified	Unclassified	55	$3.00

*For sale by the Clearinghouse for Federal Scientific and Technical Information
Springfield, Virginia 22151

FOREWORD

This report was prepared under Contract No. NASW-1785 for NASA Headquarters, Office of Advanced Research and Technology, Research Division, under the technical direction of Mr. I.R. Schwartz. The work was conducted at the Mechanical Engineering Laboratory, General Electric Research and Development Center in Schenectady, New York.

SUMMARY

Surface heat transfer rates were measured on a sharp flat plate at zero angle of attack in a hypersonic shock tunnel at flow Mach numbers of 19.2 and 25.4. The density and Knudsen number were altered to span the continuum to near free molecule flow regimes. For both Mach numbers, the heat transfer data agreed reasonably well with the strong interaction predictions of Li and Nagamatsu for Reynolds number per inch greater than 10^4 and leading edge Knudsen numbers less than 4. Below a unit Reynolds number of 10^4 a systematic reduction in the heat transfer rate close to the leading edge was observed for both Mach numbers. Furthermore, the Stanton number remained relatively constant independent of Mach number and unit Reynolds number.

TABLE OF CONTENTS

LIST OF FIGURES

LIST OF FIGURES (Continued)

LIST OF SYMBOLS

C_h	heat transfer coefficient (Stanton Number)
C_p	specific heat at constant pressure
D	coefficient from Ref. 11
E	voltage
H	enthalpy
I	current
k	thermal conductivity
Kn	Knudsen number
M	Mach number
P	pressure
q	heat transfer rate
R	resistance or gas constant
Re/in	unit Reynolds number
Re_x	length Reynolds number
$S'(0)$	coefficient from Ref. 38
t	leading edge thickness or time
T	temperature
u	velocity
$\overline{v}$	average molecular velocity
$\overline{V}_\infty$	rarefaction parameter
α	gage resistivity
β	gage backing material constant
γ	ratio of specific heats
θ	collision frequency
λ	mean free path

μ	viscosity
ν	kinematic viscosity
ξ	time for one molecular collision
ρ	density
τ	variable of integration
χ	strong interaction parameter

Subscripts

a	conditions after a normal shock
b	gage backing material or conditions before a normal shock
o	initial conditions
f	final conditions
w	wall conditions
w,i	insulated wall conditions
l	leading edge conditions
5	stagnation conditions

1.0 INTRODUCTION

The development of future hypersonic manned vehicles requires the knowledge regarding the local heat transfer rates for lifting surfaces during re-entry and cruise flights at hypersonic velocities at high altitudes. For these future hypersonic vehicles the flight Mach number will be in the range of 6 to 26 and altitudes of 10 to 60 miles. Also, the study of the rarefied gas flows for a sharp flat plate in the transition from a continuum thin boundary layer with no slip at the surface to the limiting case of free molecule flow is of great interest in gas dynamics. Only limited experimental and theoretical references are available on the rarefied flow phenomena and the available references are not adequate for predicting accurately the surface pressures, local heat transfer rates, and the shock wave and viscous layers for a given lifting surface operating in the rarefied hypersonic flight regimes.

The formation of the shock wave and boundary layer on a sharp flat plate at hypersonic Mach numbers for different rarefied flow conditions has been investigated in different types of facilities by various investigators[1-8]. It was observed experimentally in rarefied hypersonic flows that at the leading edge of a sharp flat plate there is a region of non-continuum flow and the length of this region is dependent upon the free stream Mach number and the low density condition or the mean free path ahead of the leading edge. After this initial region the shock wave and the boundary layer are merged as postulated initially by Shen[9] and Li and Nagamatsu[10,11] with the slip flow existing at the surface of the plate. Beyond this region the shock wave and boundary are still merged with no slip at the surface which corresponds to the strong interaction region as initially solved by Li and Nagamatsu[10] and later by Lees[13], Cheng[14], Stewartson[15], and others[16,17]. Downstream of this region the shock wave and the boundary layer are separated and is referred to as the weak interaction region[17]. Further downstream from the leading edge with no slip at the surface, the local skin friction and heat transfer for the laminar boundary layer are predicted by Crocco[18] and Young[19] as discussed in Refs. 8 and 20.

Recent investigations of the surface pressures, local heat transfer rates, and shock wave shape for a sharp flat plate were conducted by Vidal and Bartz[8] at Mach numbers of 18 to 24 in rarefied flow conditions. At low density conditions both pressure and heat transfer data indicated large rarefied flow effects with both slip velocity and energy jump at the plate surface. McCroskey[6] studied the induced pressure and the shock wave and boundary layer formation in heated nitrogen at hypersonic Mach numbers. Impact pressure measurements in the vicinity of the leading edge region showed the formation

of the shock wave and the viscous layer. Both surface pressures and shock wave and boundary layer formation for a flat plate were obtained in a hypersonic shock tunnel by Nagamatsu and associates[4]. Both pressures and optical data indicated large rarefied flow effects at low density conditions. The schlieren photographs indicated the absence of a shock wave at the leading edge, but with the shock wave forming farther downstream.

Numerous investigators have attempted to solve the rarefied flow phenomena for hypersonic flows over a sharp flat plate with various assumptions for the flow conditions in the leading edge region. Oguchi[21] investigated the surface pressure in the leading edge region with a wedge-like viscous layer and velocity slip at the surface. The assumption of slip flow appreciably reduced the induced pressure compared to the strong interaction without slip. Recent investigations of the flow phenomena in the rarefied hypersonic flow were conducted by Charwat[22], Chow[23], Shorenstein and Probstein[24], Rudman and Rubin[25], Huang[26], Bird[27], and Eilers[28]. In Ref. 8 the authors compared the experimental results for a flat plate with some of these recent theoretical predictions.

The purpose of this report is to present the local heat transfer rates on a flat plate with sharp and blunt leading edges in the transition from the strong interaction boundary layer regime with no slip at the surface to the free molecule regime. In the previous paper[4] the results for the surface induced pressures and the schlieren photographs of the shock wave and boundary layer formation in the vicinity of the leading edge for the same test conditions were presented. For these investigations in the hypersonic shock tunnel the nominal free stream Mach numbers were 19.2 and 25.4 with a reflected stagnation temperature of approximately 2340°R. The local heat transfer rates were determined by the use of fast response sputtered platinum heat gages, and the local heat transfer data for a flat plate with sharp and blunt leading edges are presented and compared with the strong interaction and free molecule predictions. From these comparisons the initial transition from the strong interaction region with no slip at the surface to the rarefied flow region is determined.

2.0 EXPERIMENTAL APPARATUS

2.1 Hypersonic Shock Tunnel and Instrumentation

The tests were conducted in the straight-through test section of a multiple nozzle, combustion driven shock tunnel. A reflected-type conical nozzle[29,30] with a half-angle of 15° and an exit diameter of 24 inches was used at the end of a 4 inch inside diameter, 103 foot long driven tube. A Berkeley counter was used to measure the shock velocity over a 2.5 foot section of the driven tube just ahead of the reflected nozzle. Two nozzle throats were used, 0.1 and 0.19 inch diameter, to give a nominal Mach number of 25 and 19 at the nozzle exit. A scored aluminum diaphragm at the nozzle entrance bursts with the arrival of the incident shock wave, and the flow exhausts into a 200 cubic foot dump tank which was initially evacuated to approximately 3 microns of mercury to facilitate flow establishment and minimize starting shocks.

The model was mounted on a hollow sting independently supported and isolated from the dump tank and floor. The electrical leads from the gages in the model were brought out through the sting to oscilloscopes. A detailed description of the shock tunnel and general instrumentation is presented in Refs. 29 and 31.

2.2 Flat Plate Model

The steel flat plate model, Fig. 1, used for the heat transfer investigations was 10 inches wide and 16 inches long. Thin side plates were attached to the plate to minimize the affect of any disturbance from the impact pressure gage mounted beneath the plate on the heat transfer measurements on the plate surface. The thickness of the leading edge could be varied, and leading edge thicknesses of 0.001 and 0.010 inch were used in the present investigation.

Twelve heat transfer gages were located along the center of the plate at the following distances from the leading edge: 0.19, 0.405, 0.590, 0.780, 1.10, 1.41, 2.35, 4.02, 5.56, 8.10, 10.48, and 12.94 inches. The heat transfer gages were made of platinum[3,31] sputtered on a Pyrex backing to a thickness of approximately 350Å and insulated by a silicone dioxide film. The impact pressure in the plane of the leading edge was measured with a Kistler quartz piezoelectric pressure transducer or, at the lower pressures, a lead-zirconate-titanate compensated piezoelectric gage. Each gage was placed in a cylindrical housing with a hemispherical nose. Both heat gages and impact pressure gages were dynamically calibrated in the 8-in. diameter calibration shock tube[31], before and after the present series of tests. The model was mounted in the center of the conical nozzle near the exit.

3.0 DATA REDUCTION

3.1 Determination of Test Conditions

The flow conditions in the test section are determined by the nozzle area ratio and the condition of the gas behind the reflected shock wave at the nozzle entrance. The pressure, P_5, behind the reflected shock wave was measured with a standard Kistler quartz gage, and the corresponding reflected stagnation temperature, T_5, was calculated using the known shock velocity at the end of the driven tube and the equilibrium thermodynamic properties for air[32-36]. The reflected pressures were high enough to have nearly equilibrium conditions before the gas was expanded in the nozzle.

The experiments were conducted over a range of P_5 from 50 to 2400 psia and T_5 from 2270 to 2540°R. Under these conditions nonequilibrium effects in the nozzle expansion can be neglected[30,37]. The leading edge impact pressure was used to define the leading edge Mach number using the real gas properties through the normal shock wave. Conditions at the plate leading edge and along the plate were calculated by assuming an isentropic expansion of a nonperfect gas. The nozzle angle was corrected to account for boundary layer development by using the measured impact pressure to define an effective area ratio. The calculation assumed that the presence of the plate did not effect the nozzle flow.

Since the nozzle exit is 24 inches in diameter and the throat is either 0.1 or 0.19 inches, the model will experience source flow effects where free stream conditions will vary along the plate. Calculations based on an isentropic expansion showed that over the first 13 inches of the plate where the heat transfer gages were mounted, the Mach number varied from 19 to 21 for the Mach 19 tests and from 25 to 28 for the Mach 25 tests. As a consequence, the data is presented in two ways - one where the parameters are based on free stream conditions at the given location along the plate and the other where the parameters are based on leading edge conditions, subscripted 1. This permits an analysis of the source flow effects on the plate surface heat transfer. It should be noted that in the region of the leading edge where the transition from free molecule to continuum flow occurs, the free stream properties do not vary significantly. Hence, the source flow characteristics of the nozzle should have little effect on the leading edge flow development.

3.2 Heat Transfer Gage Data Analysis

The platinum film on the backing material of the heat transfer gage is thin enough such that the thermal effects of the platinum can be neglected in comparison to the backing material. Furthermore, the backing material can be treated as a semi-infinite solid having the property $\beta_b = (\rho C_p k)_b$,

where ρ, C_p, and k are the density, specific heat, and thermal conductivity of the backing material respectively.

The change in the gage resistance, ΔR, due to a surface temperature change, $\Delta T = T_f - T_o$, is

$$\Delta R = R_f - R_o = R_o \alpha \Delta T, \tag{1}$$

where R_o and R_f are the gage resistances at temperatures T_o and T_f, and α is the resistivity. The gage is operated at a constant current I and hence the voltage change ΔE across the gage for a temperature change ΔT is

$$\Delta E = I \Delta R = I R_o \alpha \Delta T \tag{2}$$

When $\Delta T = \Delta T(t) = \Delta E(t)/\alpha I R_o$ is a function of time, the heat transfer q(t) to the gage is given in Ref. 38 as

$$q(t) = \frac{\sqrt{\pi \beta_b}}{2\alpha I R_o} \left[\frac{\Delta E(t)}{\sqrt{t}} + \frac{1}{\pi} \int_0^t \frac{\sqrt{\tau/t}\, \Delta E(t) - \Delta E(\tau)}{(t-\tau)^{3/2}} d\tau \right] \tag{3}$$

The heat transfer rate can be calculated from Eq. (3) using the voltage-time trace of the gage when the values of β_b and α are known. The constant coefficient $\sqrt{\beta_b}/\alpha$ for each gage can be obtained by a dynamic calibration.

To find the coefficient, the gages were mounted in the flat plate and placed in the center of an eight inch diameter calibrating shock tube[31]. A piece of plexiglass which extended 8 inches forward from the leading edge and from the plate edges to the tube walls was used to produce surface conditions for the gages which simulate a plate of infinite extent. When the shock passes over the plate a boundary layer forms behind the shock and there is a small step rise in the gage surface temperature evidenced by the voltage-time traces of the gage. The change in temperature is generally .1 to .2°C which is small compared to the plate surface temperature of approximately 300°K but adequate enough to give a voltage change of approximately .1 to .2 millivolts. For a step rise in temperature, the heat transfer rate $q_b(t)$ for the assumed semi-infinite solid backing material is

$$q_b(t) = \left(\frac{\beta_b}{\pi}\right)^{1/2} \frac{\Delta T}{\sqrt{t}} = \left(\frac{\beta_b}{\pi}\right)^{1/2} \frac{\Delta E}{\alpha I R_o \sqrt{t}} \tag{4}$$

For a constant wall temperature, T_w, the local heat transfer rate q(t) at the wall from the gas in the boundary layer formed by a normal shock passage over a plate is given by[39]

$$q(t) = -k_w \sqrt{\frac{u_a}{2\, u_b t \nu_w}}\, (T_w - T_{w,i})\, S'(0) \tag{5}$$

where k_w and ν_w are the gas conductivity and kinematic viscosity at the wall temperature, $T_{w,i}$ is the insulated wall temperature, u_b and u_a are the free stream velocities before and after the normal shock, and $S'(0)$ is a coefficient tabulated in Ref. 39.

Since at the gage surface $\Delta T << T_w$, the gage surface temperature changes have a negligible effect on the heat transfer rate q(t). Furthermore, since the effect of the shock passage on the gage is to give a step rise in the surface temperature, Eq. (4) and (5) can be equated and the gage coefficient $\sqrt{\beta_b}/\alpha$ can be found by

$$\frac{\alpha}{\sqrt{\beta_b}} = \frac{\Delta E}{IR_o k_w (T_w - T_{w,i}) \sqrt{\frac{\pi u_a}{2\, u_b \nu_w}}\, S'(0)} \tag{6}$$

The constants associated with the gas are accurately known and depend only on the wall temperature.

The heat transfer gages were calibrated in this manner over a shock Mach number range of 1.5 to 3, with the actual pressure rises on the surface of the plate corresponding to the estimated pressure rises that the plate would experience in the actual test section flows. This permitted the gage calibration to absorb any strain gage effects that the thin platinum film might exhibit under pressure loading.

3.3 Viscosity and Knudsen Number

The local static temperature in the vicinity of the plate was 20 - 40°R for all tests, and over this temperature range the viscosity was assumed to be a linear function of temperature. The mean free path at the plate leading edge λ_1 was determined by[40]

$$\lambda_1 = \frac{\mu_1}{0.499\, \rho_1\, \bar{v}_1} \tag{7}$$

where $\bar{v}_1$, is the average molecular velocity given by

$$\bar{v}_1 = \left(\frac{8RT_1}{\pi}\right)^{1/2} \tag{8}$$

The Knudsen number Kn_1 is defined as the ratio of the mean free path to the leading edge thickness t,

$$Kn_1 = \frac{\lambda_1}{t} \tag{9}$$

It was shown in Ref. 12 from the kinetic theory standpoint that the distance traveled along the plate for a time of one intermolecular collision in the free stream is given by

$$\xi_1 = M\lambda_1 \tag{10}$$

4.0 RESULTS

Basically the heat transfer on a flat plate was investigated at two nominal leading edge Mach numbers, 19 and 25, with the reservoir temperature fixed at approximately 2340°R. The reservoir pressure was systematically reduced to rarify the air in the test section. Tables I and II present the test conditions and the leading edge conditions for each test.

The local heat transfer rates were calculated by numerically integrating the voltage-time trace for each gage using Eq. (3). These rates are presented in Figs. 2 and 3 plotted as a function of the distance from the leading edge for the Mach 19.2 and 25.4 tests. In all cases the ratio of the wall temperature to free stream stagnation temperature is approximately 0.235 ($T_w \cong 540°R$). For the high density flow conditions with corresponding large unit Reynolds numbers, the local heat transfer rates for both Mach numbers increase monotonically towards the leading edge of the flat plate as predicted by the strong interaction theory of Li and Nagamatsu[11] for a cooled wall with no slip flow at the surface. Under these conditions the leading edge rarefied flow effects are small compared to the strong shock wave boundary layer interaction with zero velocity at the surface. Similar results were indicated by the surface induced pressures and schlieren photographs of the shock wave and boundary layer formation in high density flows as discussed in Ref. 4.

As the Knudsen number increases and the Reynolds number per inch decreases, the heat transfer rate in the vicinity of the leading edge diminishes, and at the very low unit Reynolds number the heat transfer is nearly constant along the entire length of the plate. The mean free path for the low unit Reynolds number tests is approximately 0.06 inches, the free stream velocity is approximately 5500 ft/sec., and the gas temperature is of the order of 36°R. Hence, the molecular collision frequency, $\theta_1 = \bar{v}_1/\lambda_1$, is approximately 6×10^5 collisions per second. With the molecules traveling at 5500 ft/sec. they then travel on the average 0.12 inches along the plate between collisions. There are not enough collisions in the vicinity of the leading edge to permit a boundary layer or shock wave formation and a region of rarefied flow appears. Further downstream, after more collisions the boundary layer and shock wave develop. The consequence of this flow development is a reduction in the energy transferred to the plate at the leading edge as exhibited in Figs. 2 and 3 and indicated in Refs. 21 - 27. In Figs. 4a - d the local heat transfer rates normalized by the free stream kinetic energy are presented as a function of the mean free paths along the plate for the two Mach numbers investigated. Since the flat plate was tested at the exit of the conical nozzle, the free stream kinetic energy was taken to be either

the value at a given location on the plate to account for source flow, or the value existing at the leading edge of the plate. In Figs. 4a and 4b the Mach 19.2 and 25.4 data respectively are presented where the flow conditions, ρ, u, M, μ, and T are local conditions along the plate. As a comparison, Figs. 4c and 4d present the same results except that the flow conditions are based on the leading edge conditions, ρ_1, u_1, M_1, μ_1, and T_1. At the leading edge the nondimensionalized heat transfer rates obtained by the two normalizing methods yield the same result, but for locations farther downstream from the leading edge the use of local conditions as flow conditions should be more accurate than using the leading edge conditions. As can be seen from these figures there is little difference between the data with these two conditions even at the plate trailing edge. For all of the test conditions at Mach numbers of 19.2 and 25.4, the scatter in the data for distances greater than 100 mean free paths from the leading edge is quite small. But for distances closer to the leading edge there is appreciable differences for lower unit Reynolds numbers.

If the flow is truly free molecule with diffuse reflection, the heat transfer would be constant along the plate as indicated in Ref. 41 and in these figures. The relation for large Mach numbers for perfectly diffuse reflection is

$$\frac{2q}{\rho u^3} \cong \frac{1}{\sqrt{2\pi\gamma}\, M} \tag{11}$$

where γ is the ratio of specific heats, 1.4 for air. For all the tests at both Mach numbers, the lowest density tests exhibited a relatively constant heat transfer rate over 10 - 30 mean free paths from the leading edge. Evidently the flow at the leading edge for this test is approaching free molecule slip flow. Further downstream the velocity is reduced and enough collisions are occurring to permit a continuum, no-slip flow development.

At present there are many theories that treat the hypersonic leading edge problem[10] in the free molecule to continuum flow regime[21-26]. Some of these theories treat the problem from a kinetic theory point of view[22,27] and some treat it as a continuum problem by introducing a slip condition at the wall near the leading edge. None of these theories are reasonably simple for a quick comparison with experimental data. In Ref. 8 some of these theories have been compared with the experimental flat plate surface measurements.

The strong interaction theory of Ref. 11 provides simple relationships for deciding whether the flow at a particular

location along the plate is a continuum shock wave boundary layer interaction or transitional from free molecule to continuum. Both surface pressure and heat transfer along the plate agree reasonably well with the strong interaction theory when there is no slip flow at the leading edge[1-8]. The heat transfer coefficient C_h for the strong interaction theory[11] is given by

$$M^3 C_h = D \left(\frac{M^3}{\sqrt{Re_x}} \right)^{3/2} \tag{12}$$

where

$$C_h = \frac{q}{\rho u (H_5 - H_w)} \equiv \text{Stanton number}$$

H_5 = stagnation enthalpy

H_w = wall enthalpy

$Re_x = \frac{\rho u x}{\mu}$ = length Reynolds number

The expression for $D = f(\gamma, T_w/T_5)$ and its values are presented in Ref. 11.

Figs. 5a - d present the results of the heat transfer correlation based on Eq. (12) for the Mach 19.2 and 25.4 tests. Both local conditions from the source flow and conditions at the plate leading edge were used for the correlation. The use of the local conditions for correlation with the strong interaction theory for heat gages located farther downstream from the leading edge gives better agreement for both free stream Mach numbers as indicated in Figs. 5a and 5b than using the leading edge flow conditions, Figs. 5c and 5d. For the Mach 19.2 tests at values of the interaction parameter, $\chi = M^3/\sqrt{Re_x}$ greater than 100, the heat transfer rates depart from the strong interaction predictions. For interaction parameters greater than 100, the local heat transfer rates are much less than that predicted by the theory with no slip flow at the surface. At the lowest unit Reynolds number of 422 and leading edge Knudsen number of 67.6 the local heat transfer rate at the first heat gage location of 0.19 in. from the leading edge is approximately an order of magnitude less than that predicted by the strong interaction theory.

For a given Mach number the data correlates well over the entire flow regime; however, the departure from the strong

interaction is a function of flow Mach number. For the Mach 25.4 tests, Fig. 5b, this departure occurs due to the rarefied flow effects for values of χ greater than 300. Again for the lowest density conditions with unit Reynolds number of 542 and leading edge Knudsen number of 62.1, the local heat transfer rates over the front part of the flat plate were approximately an order of magnitude less than that predicted by the strong interaction theory with no slip flow at the surface. Thus, the rarefied flow effects at Mach numbers of 19.2 and 25.4 produce a large decrease in the local heat transfer rates for a sharp flat plate. In previous investigations[1-4] with a sharp flat plate the local heat transfer rates and induced pressures were found to be lower than the predictions of the strong interaction theory[10,11] at hypersonic Mach numbers. Other investigators[5-8] have observed the large reductions in the heat transfer rates and induced pressures for rarefied hypersonic flows.

The parameter M^3C_h is plotted against the rarefaction parameter, $\bar{V}_\infty = M/\sqrt{Re_x}$, in Figs. 6a and 6b with local conditions and in Figs. 6c and 6d with leading edge conditions. In these figures the free molecule prediction for diffuse reflection at the plate surface is shown for free stream Mach numbers of 19.2 and 25.4. Departure from the strong interaction theory with no slip flow occurs at $\bar{V}_\infty \cong 0.25$ for the Mach 19.2 tests and at $\bar{V}_\infty \cong 0.45$ for the Mach 25.4 tests. For both Mach numbers the local heat transfer rates are larger than the values for free molecule flow with diffuse reflection. At the lowest density flow conditions for a Mach number of 19.2 the rarefaction parameter for the first heat gage location was approximately 2 and the local heat transfer rate was an order of magnitude less than that for the strong interaction prediction. But for the highest density condition with unit Reynolds number of 22,711 and leading edge Knudsen number of 1.26, the local heat transfer rates over the plate surface were close to the strong interaction prediction with the slope slightly less than the theoretical value as indicated in Figs. 6a and 6c.

For a flow Mach number of 25.4 the highest unit Reynolds number was 9,758 and for this condition the local heat transfer parameter as a function of the rarefaction parameter was close to that predicted by the strong interaction theory with the slope slightly less than the theoretical value as indicated in Figs. 6b and 6d. But for the lowest density condition with unit Reynolds number of 542 and leading edge Knudsen number of 62.1, the rarefaction parameter was approximately 2 at the first heat gage location, and the local heat transfer rate was an order of magnitude less than the strong interaction value with no slip flow at the plate surface. Even for this value for the rarefaction parameter the local heat transfer rate is much larger than the free molecule

value with diffuse reflection at the surface. Similar results were recently obtained in Ref. 8 for a sharp flat plate in hypersonic flows with higher stagnation temperatures than that used in the present investigations.

The dependence of the heat transfer coefficient on Mach number and Reynolds number can be removed in the strong interaction regime by dividing M^3C_h by $\chi^{3/2}$ as seen from Eq. (12). Any departure from a constant value of $M^3C_h/\chi^{3/2}$, which depends upon the ratio of the specific heats for the gas and the ratio of the wall to stagnation temperatures, indicates a departure from the heat transfer rate governed by the strong interaction flow with no slip flow at the surface. It is also interesting to note that the constant value of $M^3C_h/\chi^{3/2}$ is independent of the flow Mach number in the hypersonic continuum flows. This parameter is plotted in Figs. 7a - d as a function of the rarefaction parameter based on the local and leading edge conditions for Mach 19.2 and 25.4 tests. Also, in these figures the curves for the conditions of free molecule flow with diffuse reflection are presented for the highly cooled wall case, with a sharp leading edge. At low density conditions the slope of the experimental heat transfer data are close to that for the free molecule flow conditions for both Mach numbers of 19.2 and 25.4.

Similar results were observed by Vidal[8] at lower density conditions and corresponding higher values for the rarefaction parameter at a free stream Mach number of approximately 20. These results were obtained with the wall to stagnation enthalpy ratio of .064, which is much lower than the value for the present investigation. For a rarefaction parameter, $\bar{V}_\infty$, of approximately 6 and unit Reynolds number of 370 the local heat transfer rate measured by Vidal was close to the free molecule prediction with diffuse reflection. These low density conditions were not achieved in the present investigation because the stagnation temperature was approximately 2340°R in order to minimize the real gas effects.

In Fig. 8 the local heat transfer parameter $M^3C_h/\chi^{3/2}$ is presented as a function of the rarefaction parameter for all tests at Mach numbers of 19.2 and 25.4. The curves for these Mach numbers are drawn to include the spread in the experimental data. Also, the limiting curves for free molecule flow conditions are presented for both Mach numbers. The experimental data covers approximately a 40 to 1 range in the strong interaction parameter, χ, leading edge Knudsen number, Kn_1, unit Reynolds number based upon the leading edge conditions, Re_1/in, and the rarefaction parameter, $\bar{V}_\infty$. For each Mach number the spread in the data is reasonably small, but there is a Mach number dependency in this correlation. A large portion of the heat transfer data for

both Mach numbers are believed to be representative of heat transfer rates on a flat plate with sharp leading edge in continuum to free molecule transitional flow. For high density hypersonic flows with low values for the rarefaction parameter, the local heat transfer rates are slightly higher than the values predicted from the strong interaction theory[11] with no slip flow. Based on the diffuse free molecule flow limit predictions, for the present investigation none of the heat transfer rates were obtained in truly free molecule flow.

Both leading edge Knudsen number and unit Reynolds number play a role in the shock wave and boundary layer formation in the vicinity of the leading edge. Small Knudsen numbers correspond to a blunt leading edge with a detached shock wave and viscous effects are small for this condition. Small unit Reynolds numbers and large Knudsen numbers correspond to highly rarefied flow where slip flow occurs at the leading edge and the shock wave-boundary layer formation is delayed. By changing the plate leading edge thickness from .001 to .010 in., the Knudsen number was changed by a factor of 10 while the unit Reynolds number was held fixed. Fig. 9 presents the results of these tests for moderate unit Reynolds numbers where it is seen that for a leading edge thickness of 0.010 inch the heat transfer at the first gage is slightly higher compared to the heat transfer for a plate with a leading edge thickness of 0.001 inch. For these moderate unit Reynolds number conditions the plate looks sharp to the flow with the rarefaction effects dominating the leading edge bluntness effect[42].

In a similar manner the effect of unit Reynolds number on the flow development can be determined by holding the leading edge Knudsen number constant. Fig. 10 presents the effect on the heat transfer for a 14 to 1 change in unit Reynolds number at a fixed Knudsen number. For the high unit Reynolds number of 22,700, all the data points for all the heat transfer gages along the plate agree with the strong interaction theory. However, at the lower unit Reynolds number of 1982 the heat transfer rates over a distance along the plate of approximately 2 inches from the leading edge are significantly lower than that predicted by strong interaction theory. Furthermore, from comparing the data with the diffuse free molecule flow limiting heat transfer value, the flow is believed to be transitional over these two inches. The shock wave-boundary layer begins its development a significant distance from the leading edge as discussed in Ref. 4.

The variation in the heat transfer rate close to the leading edge with unit Reynolds number is shown in Fig. 11 for all the Mach 19.2 and 25.4 tests. The heat transfer rate is measured by the gage closest to the leading edge, x = 0.19 inch. Below a unit Reynolds number of approximately 10^4, the

heat transfer rate deviates markedly from the continuum flow strong interaction analysis. In fact, M^3C_h is nearly independent of unit Reynolds number in this flow regime. It is interesting to note that the Stanton number, C_h, near the leading edge is nearly a constant independent of Mach number for unit Reynolds numbers less than 10^4. This is exemplified further in Fig. 12 where the same heat transfer data is shown as a function of leading edge mean free path λ_1. For λ_1 greater than 0.005 inches the Stanton number is a constant at this leading edge position independent of Mach number over the entire range tested for Mach numbers of 19.2 and 25.4. It is also evident in this figure that moderate leading edge bluntness effects are not large in rarefied hypersonic flow conditions.

5.0 CONCLUSIONS

Surface heat transfer rates were measured on a sharp flat plate at zero angle of attack in a hypersonic shock tunnel. The stagnation temperature was held fixed and the pressure was reduced to systematically span the continuum to near free molecule flow regimes. Two flow Mach numbers of 19.2 and 25.4 were investigated. For these conditions, the strong interaction parameter, $\chi = M^3/\sqrt{Re_x}$, varied from 20 to 1100, the leading edge Knudsen number from 1.3 to 68, and unit Reynolds number from 400 to 22,700.

Source flow effects associated with the conical nozzle of the tunnel give rise to nonconstant free stream flow conditions along the plate. This effect was investigated by correlating the heat transfer coefficient, i.e., Stanton number, using both local and leading edge conditions. The scatter in the data using local conditions was less, but both sets of data correlated reasonably well for a given Mach number.

For both Mach numbers of 19.2 and 25.4, the heat transfer data agreed reasonably well with the strong interaction prediction of Li and Nagamatsu for unit Reynolds numbers greater than approximately 10^4 and leading edge Knudsen numbers less than approximately 4. At lower density conditions the rarefied flow effects began to dominate the flow phenomena near the leading edge region of the sharp flat plate.

Leading edge bluntness up to 0.01 inch had negligible effect on the flat plate heat transfer. Both unit Reynolds number, $Re_x = \rho u/\mu$, and leading edge mean free path had a strong influence on the heat transfer close to the leading edge. A systematic reduction in the heat transfer rate close to the leading edge was observed for both Mach number tests as the leading edge density was reduced and the mean free path was increased. Below Reynolds numbers of 10^4 and above a mean free path of approximately 0.005 inch, the Stanton number remained relatively constant independent of Mach number.

REFERENCES

1. Nagamatsu, H.T. and Sheer, R.E., Jr., "Hypersonic Shock Wave-Boundary Layer Interaction and Leading Edge Slip," ARS Jour., Vol. 30, No. 5, p. 454, 1960.

2. Nagamatsu, H.T., Sheer, R.E., Jr., and Schmid, J.R., "High Temperature Rarefied Hypersonic Flow Over a Flat Plate," ARS Jour., Vol. 31, No. 7, p. 902 (1961).

3. Nagamatsu, H.T., Weil, J.A., and Sheer, R.E., Jr., "Heat Transfer to Flat Plate in High Temperature Rarefied Ultra-high Mach Number Flow," ARS Jour., Vol. 32, p. 533 (1962).

4. Nagamatsu, H.T., Wisler, D.C., and Sheer, R.E., Jr., "Continuum to Free Molecule Flow in the Vicinity of the Leading Edge of a Flat Plate at Mach Numbers of 19.4 and 24.1," Sixth International Symposium on Rarefied Gas Dynamics, Vol. I, pg. 209, Mass. Inst. Tech., July 1968.

5. Laurmann, J.A., "The Effects of Slip Flow on Induced Pressures," J. Aero. Space Sci., Vol. 26, No. 1, p. 53 (1959).

6. McCroskey, W.J., Bogdonoff, S.M., and McDougall, J.G., "An Experimental Model for the Sharp Flat Plate in Rarefied Hypersonic Flow," AIAA J., Vol. 4, No. 9, p. 1580 (1966).

7. Vidal, R.J. and Wittliff, C.E., "Hypersonic Low Density Studies of Blunt and Slender Bodies," Rarefied Gas Dynamics, Suppl. 2, Academic Press, New York (1963).

8. Vidal, R.J. and Bartz, J.A., "Surface Measurements on Sharp Flat Plates and Wedges in Low-Density Hypersonic Flow," Cornell Aero. Lab. Rept. AF-2041-A-2, (1968).

9. Shen, S.F., "An Estimate of Viscosity Effect on the Hypersonic Flow Over an Insulated Wedge," J. Math. Phys., Vol. 31, p. 192 (1952).

10. Li, T.Y. and Nagamatsu, H.T., "Shock-Wave Effects on the Laminar Skin Friction of an Insulated Flat Plate at Hypersonic Speeds," J. Aero. Sci., Vol. 20, No. 5, p. 345 (1953).

11. Li, T.Y. and Nagamatsu, H.T., "Hypersonic Viscous Flow on Noninsulated Flat Plate," Proc. Fourth Midwestern Conf. on Fluid Mechanics, Purdue Eng. Research Series No. 128, p. 273 (1955).

12. Nagamatsu, H.T. and Li, T.Y., "Hypersonic Flow Near the Leading Edge of a Flat Plate," Phys. Fluid, Vol. 3, p. 140 (1960).

13. Lees, L., "On the Boundary Layer Equations in Hypersonic Flow and Their Approximate Solutions," J. Aero. Sci., Vol. 20, No. 2, p. 143 (1953).

14. Cheng, H.K., Hall, J.G., Golian, T.C., and Hertzberg, A., "Boundary-Layer Displacement and Leading-Edge Bluntness Effects in High Temperature Flow," J. Aero. Sci., Vol. 28, p. 353 (1961).

15. Stewartson, K., "On the Motion of a Flat Plate at High Speeds in a Viscous Compressible Fluid II. Steady Motion," J. Aero. Sci., Vol. 22, No. 5, p. 303 (1955).

16. Mann, W.H. and Bradley, R.G., Jr., "Hypersonic Viscid-Inviscid Interaction Solutions for Perfect Gas and Equilibrium Real Air Boundary Layer Flow," J. Astronaut. Sci., Vol. 10, p. 14 (1963).

17. Lees, L. and Probstein, R.F., "Hypersonic Viscous Flow Over a Flat Plate," Rept. No. 195, Dept. Aero. Eng., Princeton Univ. (1952).

18. Crocco, L., "A Characteristic Transformation of the Equations of the Boundary Layer in Gases," Atti di Guidonia, No. 6, May 10, 1939, XVII. Translated in Aero. Res. Co. Rept. No. 4502, 1939.

19. Young, A.D. from Howarth, L., Modern Developments in Fluid Dynamics High Speed Flow, 1, p. 402, Oxford University Press, London (1953).

20. Nagamatsu, H.T., Wisler, D.C., and Sheer, R.E., Jr., "Hypersonic Laminar and Turbulent Skin Friction and Heat Transfer on a Slender Cone," G.E. Res. and Dev. Center Rept. 69-C-098 (1969).

21. Oguchi, H., "Leading Edge Slip Effects in Rarefied Hypersonic Flow," Rarefied Gas Dynamics, Suppl. 2, Vol. II, Academic Press, New York (1963).

22. Charwat, A.F., "Molecular Flow Study of Hypersonic Sharp Leading Edge Interaction," Rarefied Gas Dynamics, Suppl. 1, Academic Press, New York (1961).

23. Chow, W.L., "Hypersonic Rarefied Flow Past the Sharp Leading Edge of a Flat Plate," AIAA J., Vol. 5, No. 9, p. 1549 (1967).

24. Shorenstein, M.L. and Probstein, R.F., "The Hypersonic Leading Edge Problem," AIAA J., Vol. 6, No. 10, p. 1898 (1968).

25. Rudman, S. and Rubin, S.G., "Hypersonic Viscous Flow Over Slender Bodies with Sharp Leading Edges," AIAA J., Vol. 6, No. 10, p. 1883 (1968).

26. Huang, A.B. and Hwang, P.F., "The Supersonic Leading Edge Problem According to the Ellipsoidal Model," AIAA Paper No. 69-652 (1969).

27. Bird, G.A., "The Structure of Rarefied Gas Flows Past Simple Aerodynamic Shapes," J. Fluid Mech., Vol. 36, Part 3, p. 571 (1969).

28. Eilers, R.E., "Hypersonic Rarefied Gas Flow Past Two Dimensional Slender Bodies," Ph.D. Thesis, Univ. of Ill. (1969).

29. Nagamatsu, H.T., Geiger, R.E., and Sheer, R.E., Jr., "Hypersonic Shock Tunnel," ARS J., Vol. 29, No. 5, p. 332 (1959).

30. Nagamatsu, H.T., Sheer, R.E., Jr., and Workman, J.B., "Hypersonic Nozzle Expansion with Air Atom Recombination Present," J. Aero. Sci., Vol. 28, p. 833 (1961).

31. Nagamatsu, H.T., Sheer, R.E., Jr., and Weil, J.A., "Improvements in Hypersonic Technique and Instrumentation," G.E. Res. Lab. Rept. 62-RL-3107C, (1962).

32. Gilmore, F.R., "Equilibrium Composition and Thermodynamic Properties of Air to 24,000°K," Rand Rept. RM-1543 (1953).

33. Hirschfelder, J.D. and Curtis, C.F., "Thermodynamic Properties of Air," Univ. of Wisconsin, CM-518, Navy Bu. Ord. Contract No. 9938 (1948).

34. Treanor, C.E. and Logan, J.G., Jr., "Tables of Thermodynamic Properties of Air from 3000°K to 10,000°K," Cornell Aero. Lab. Rept. AD-1052-A-2 (1956).

35. Hilsenrath, J. and Beckett, C.W., "Tables of Thermodynamic Properties of Argon-Free Air to 15,000°K," Arnold Eng. Dev. Ctr. TN56-12 (1956).

36. Feldman, S., "Hypersonic Gas Dynamic Charts for Equilibrium Air," AVCO Res. Lab. Rept. (Jan. 1957).

37. Nagamatsu, H.T. and Sheer, R.E., Jr., "Vibrational Relaxation and Recombination of Nitrogen and Air in Hypersonic Nozzle Flows," AIAA J., Vol. 3, No. 8, p. 1386 (1965).

38. Carslow, H.S. and Jaeger, J.C., Conduction of Heat in Solids, University Press, Oxford (1950).

39. Mirels, H., "Laminar Boundary Layer Behind Shock Advancing into Stationary Fluid," NACA TN3401 (1955).

40. Kennard, E.H., Kinetic Theory of Gases, McGraw-Hill, New York (1938).

41. Patterson, G.N., Molecular Flow of Gases, Wiley, New York (1965).

42. Nagamatsu, H.T., Weil, J.A., and Sheer, R.E., Jr., "Leading Edge Bluntness and Slip Flow Effects in High Temperature Hypervelocity Flow Over a Flat Plate," AGARD, High Temperature Aspects of Hypersonic Flow, Chp. 35, Pergamon Press (1963).

TABLE I

CONDITIONS FOR M = 19.2 TESTS

RUN	P_5 (psia)	T_5 (°R)	T_w/T_5	Re/in	λ_1 (In. x 10^3)	L.E. Thickness (Inch)	Kn_1
1	2188	2290	0.235	22,711	1.26	0.001	1.26
2	1402	2400	0.225	15,088	1.89	0.001	1.89
3	603	2590	0.208	5,050	5.65	0.001	5.65
4	287	2290	0.235	3,077	9.27	0.001	9.27
5	189	2270	0.238	1,990	14.34	0.001	14.34
6	92	2400	0.225	924	30.88	0.001	30.88
7	51	2540	0.213	422	67.69	0.001	67.69
8	302	2400	0.225	3,039	9.40	0.01	0.94
9	186	2270	0.238	1,982	14.40	0.01	1.44

TABLE II

CONDITIONS FOR M = 25 TESTS

RUN	P_5 (psia)	T_5 (°R)	M_1	T_w/T_5	Re/in	λ_1 (in. x 10^3)	Kn_1
1	2400	2420	25.40	0.224	9,758	3.87	3.87
2	1797	2290	25.40	0.235	8,230	4.59	4.59
3	1255	2270	25.40	0.238	6,151	6.14	6.14
4	905	2380	25.40	0.227	3,664	10.31	10.31
5	600	2540	25.40	0.213	2,241	16.85	16.85
6	300	2390	25.22	0.226	1,365	27.45	27.45
7	85	2290	25.65	0.235	542	62.07	62.07

ALL 0.001 INCH LEADING EDGE

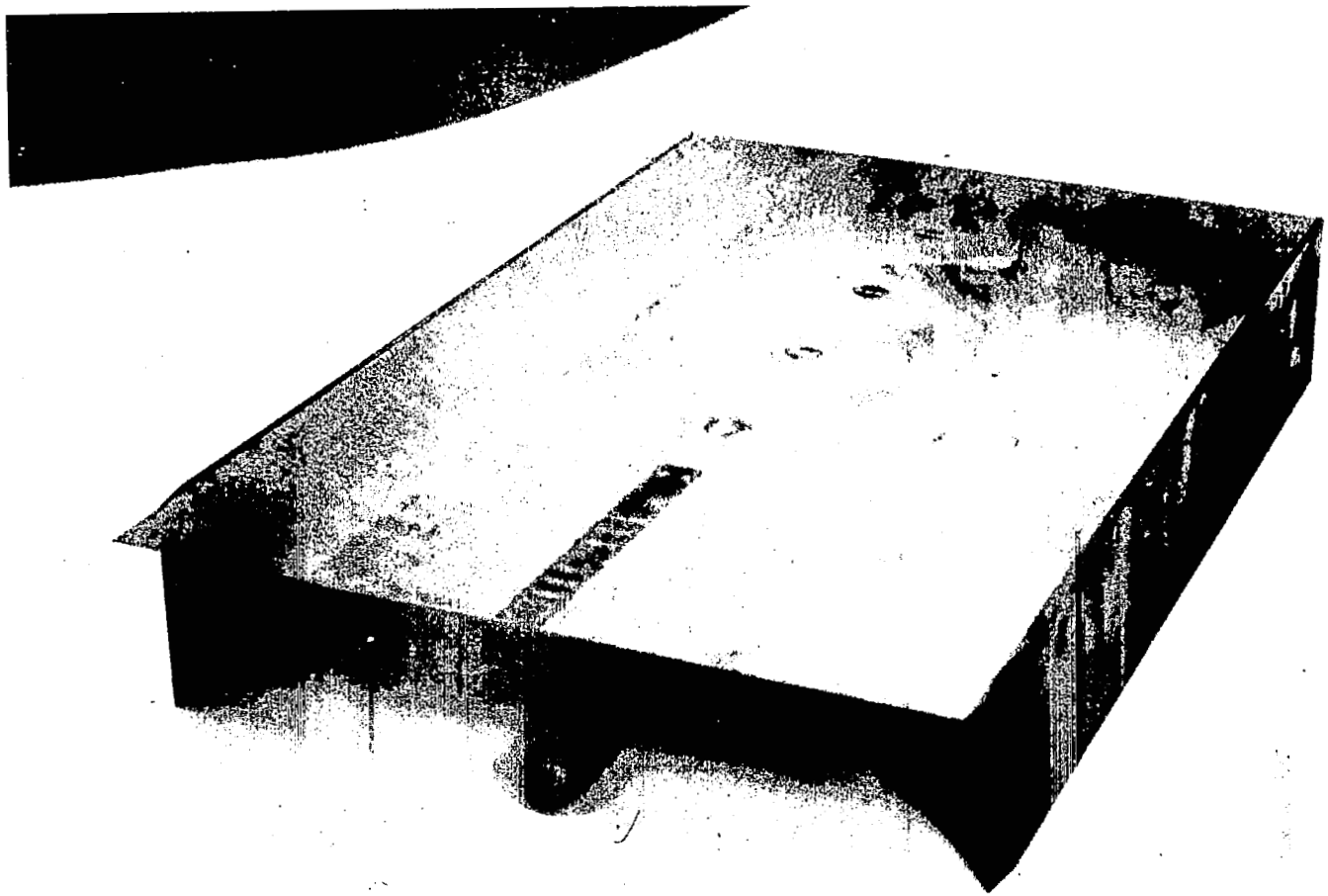

FIG. 1. FLAT PLATE HEAT TRANSFER MODEL.

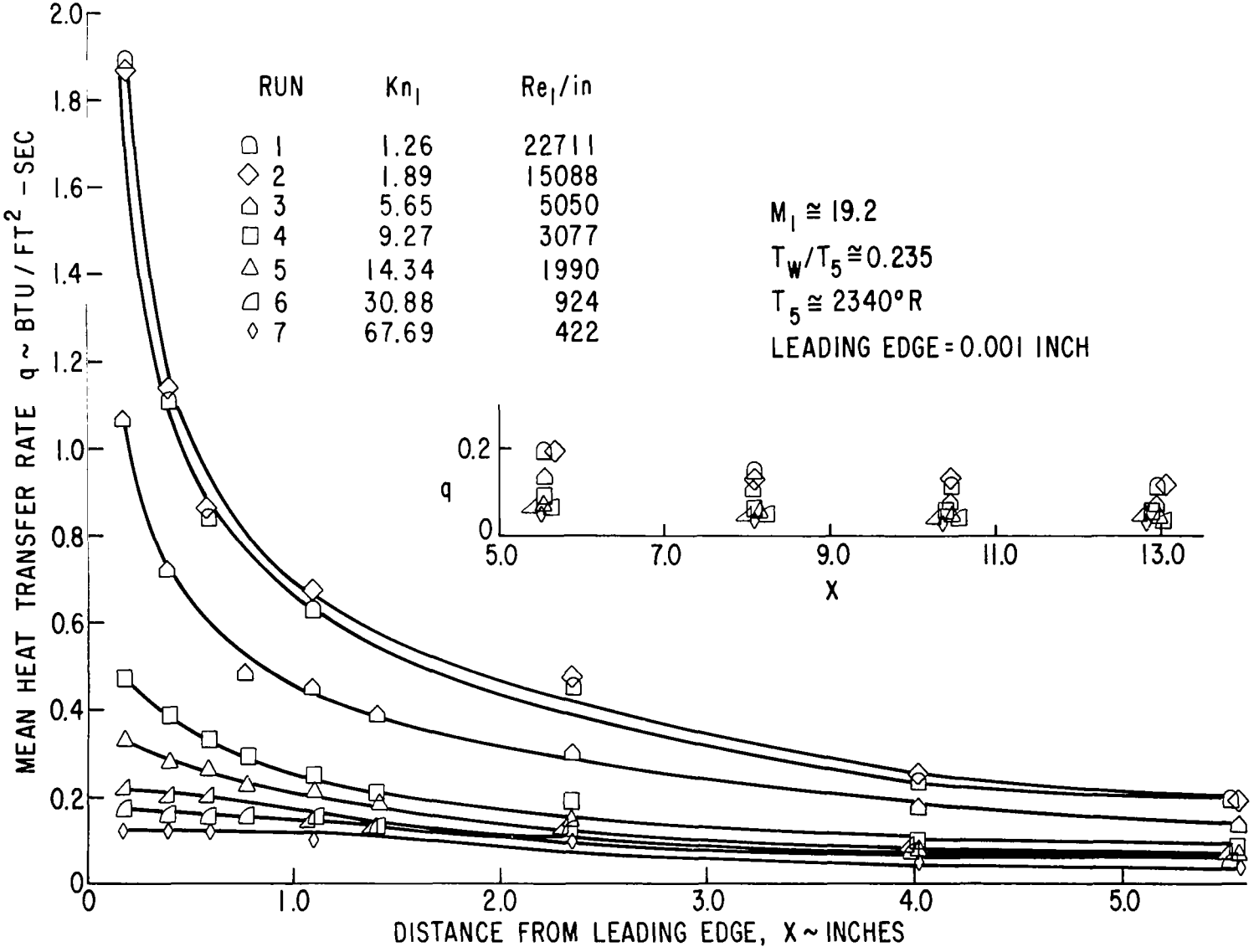

FIG. 2 HEAT TRANSFER RATE vs. DISTANCE ALONG PLATE, M ≅ 19.2.

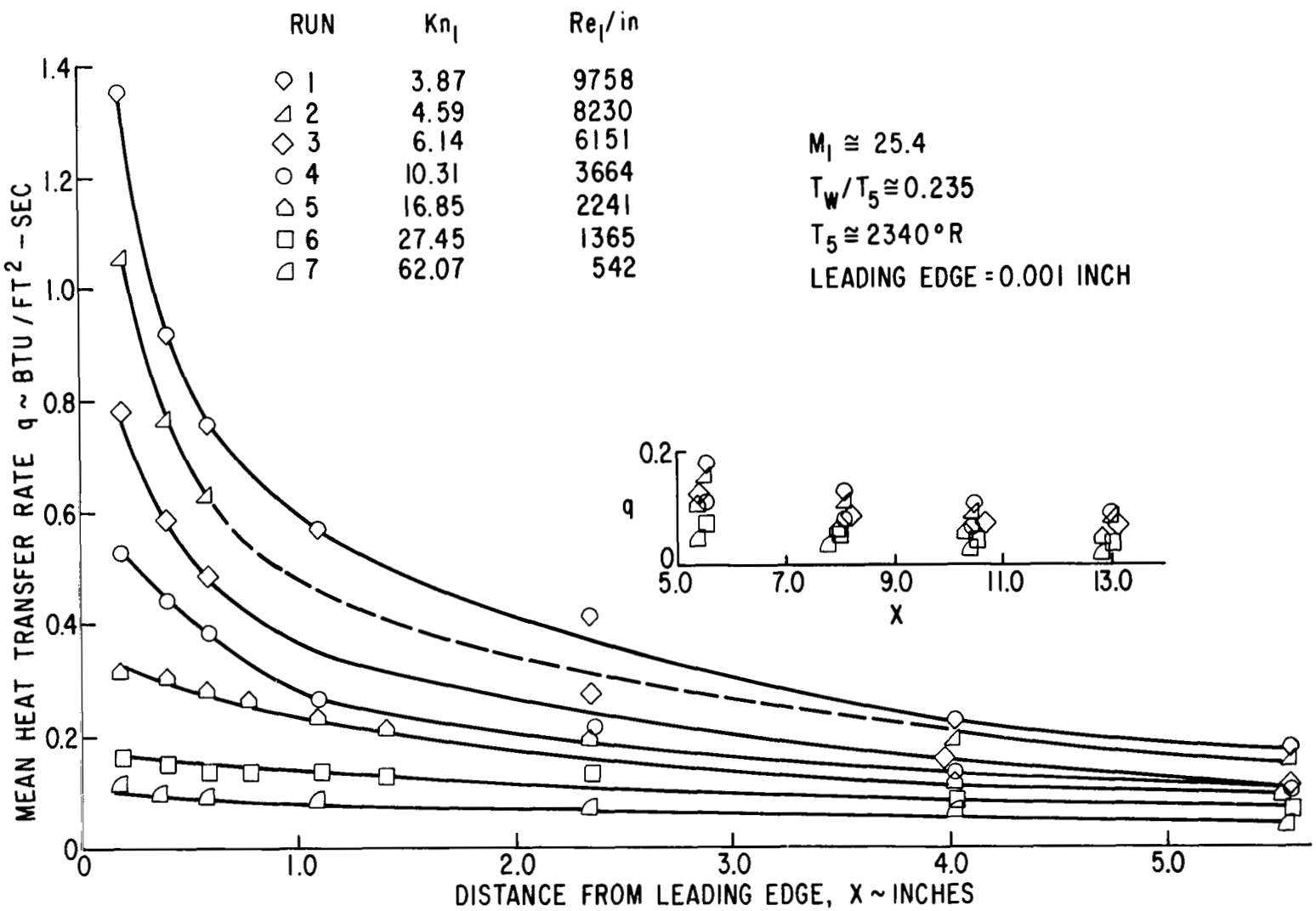

FIG. 3 HEAT TRANSFER RATE vs. DISTANCE ALONG PLATE, M≅25.4.

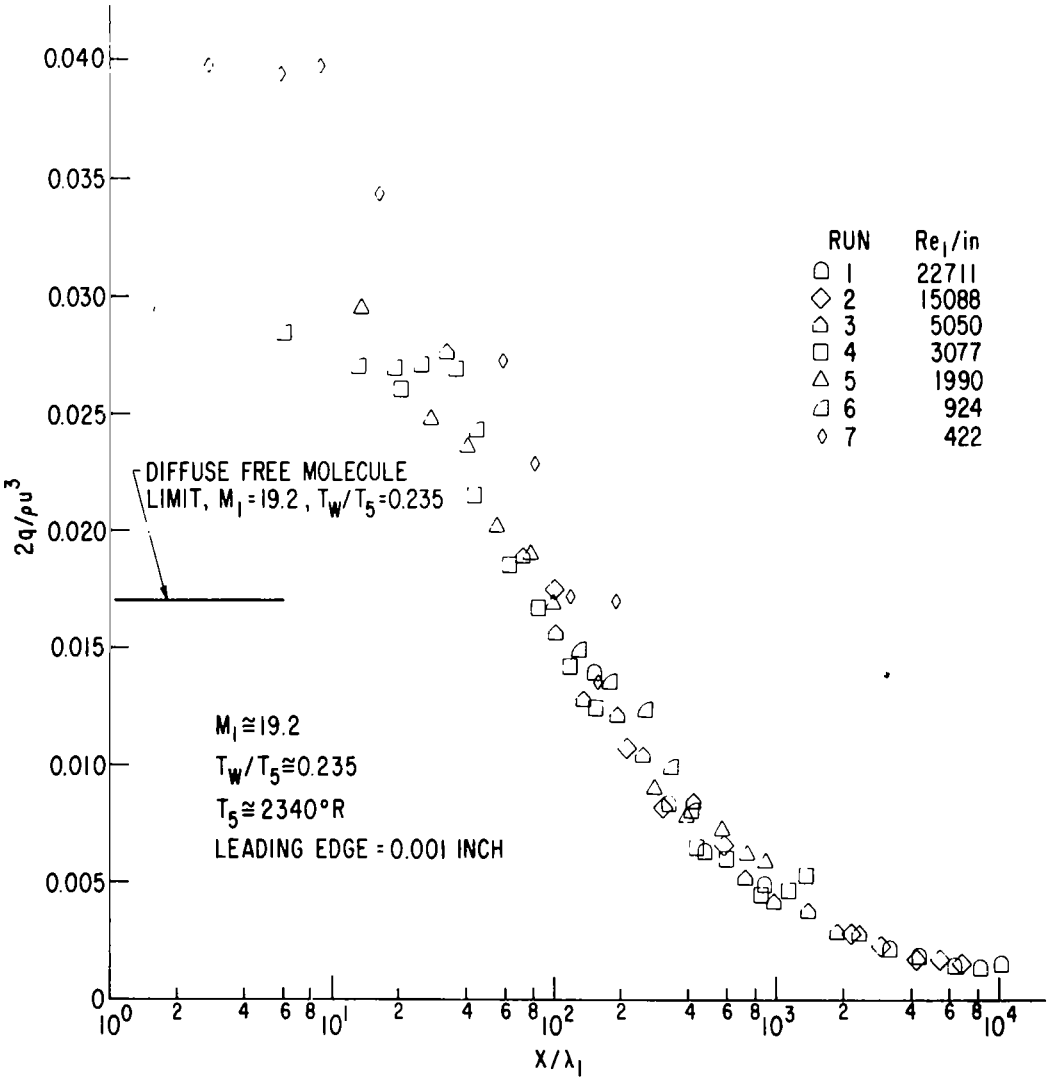

FIG. 4a NORMALIZED HEAT TRANSFER RATE vs. DISTANCE ALONG PLATE IN MEAN FREE PATHS WITH LOCAL CONDITIONS, M≅19.2.

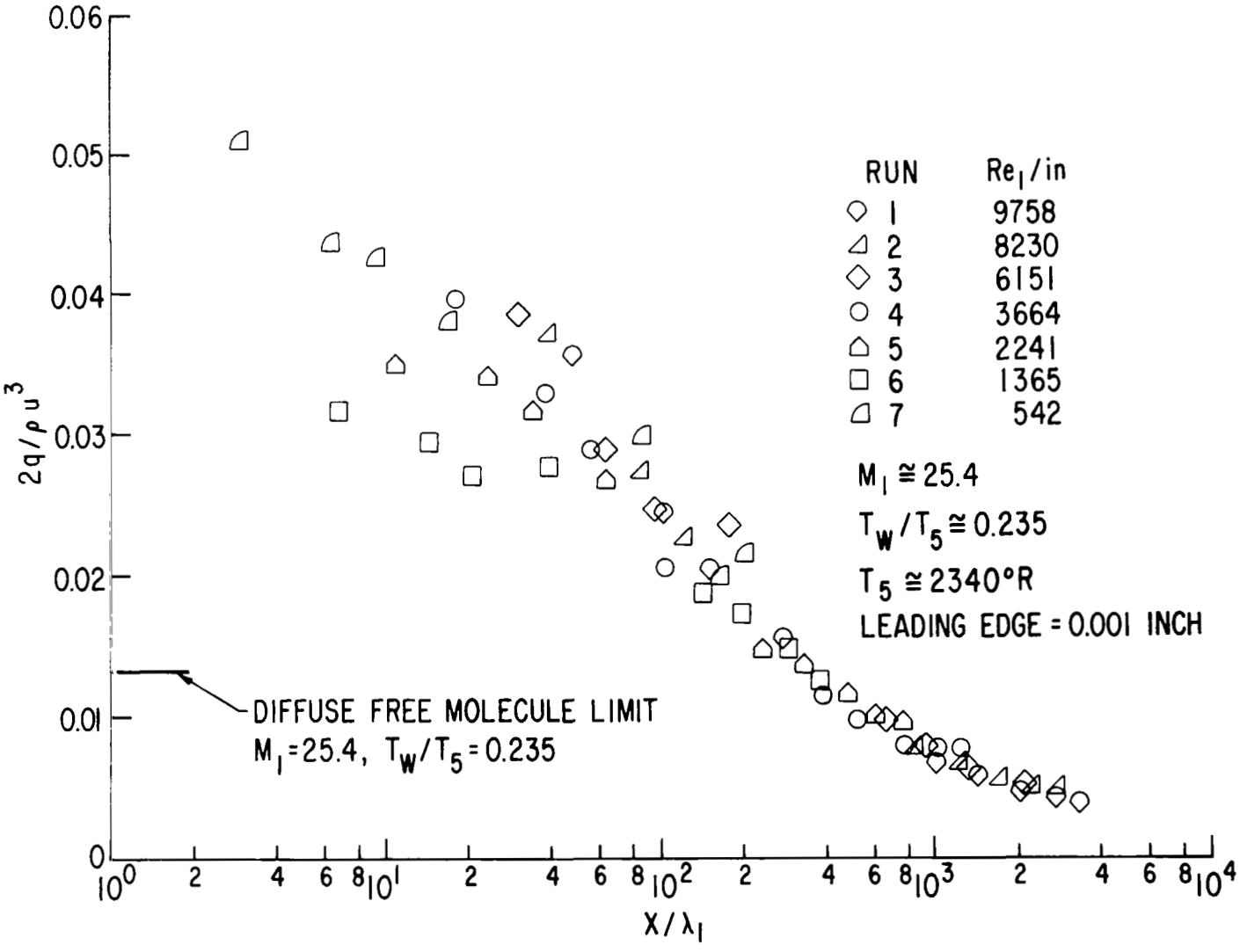

FIG. 4b NORMALIZED HEAT TRANSFER RATE vs. DISTANCE ALONG PLATE IN MEAN FREE PATHS WITH LOCAL CONDITIONS, M≅25.4.

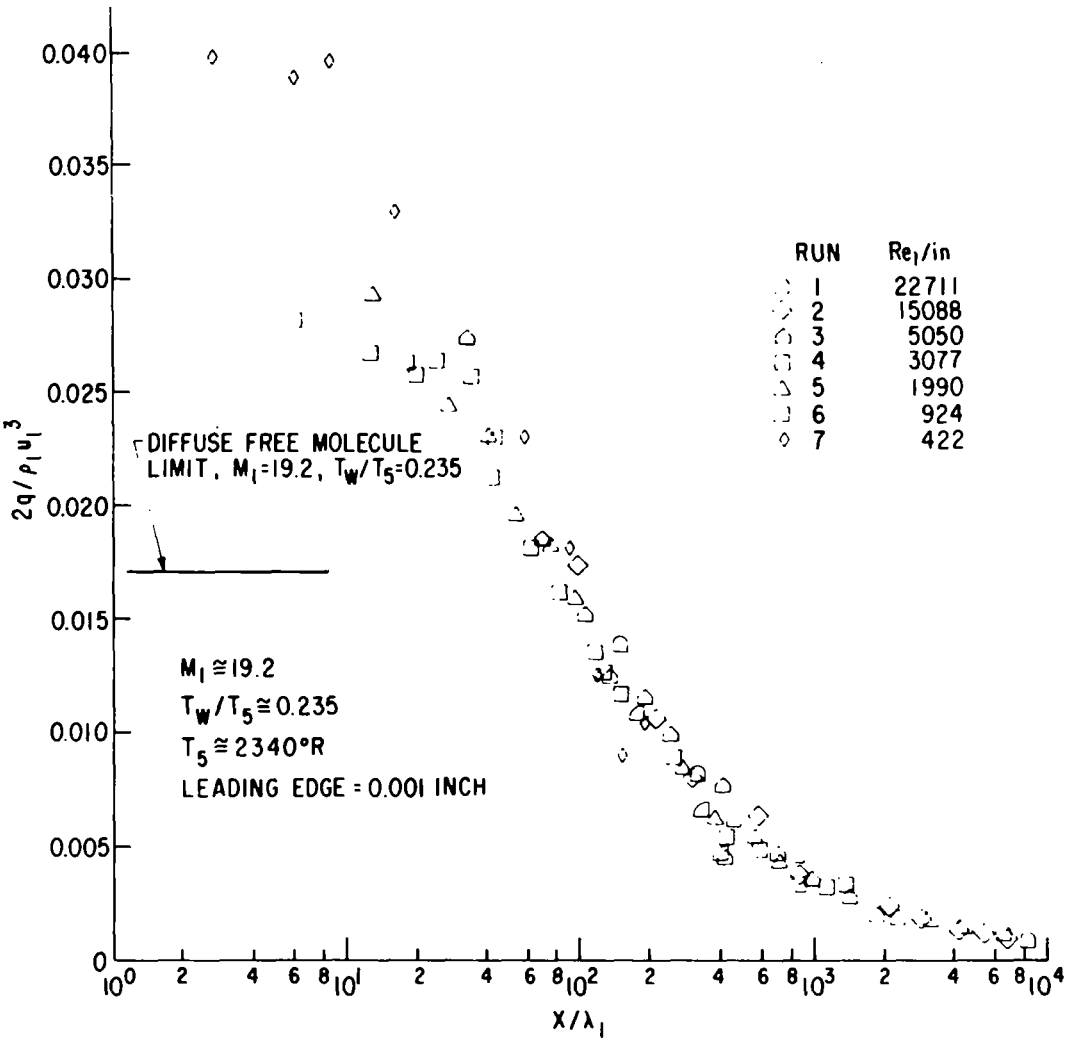

FIG. 4c NORMALIZED HEAT TRANSFER RATE vs. DISTANCE ALONG PLATE IN MEAN FREE PATHS WITH LEADING EDGE CONDITIONS, M≅19.2.

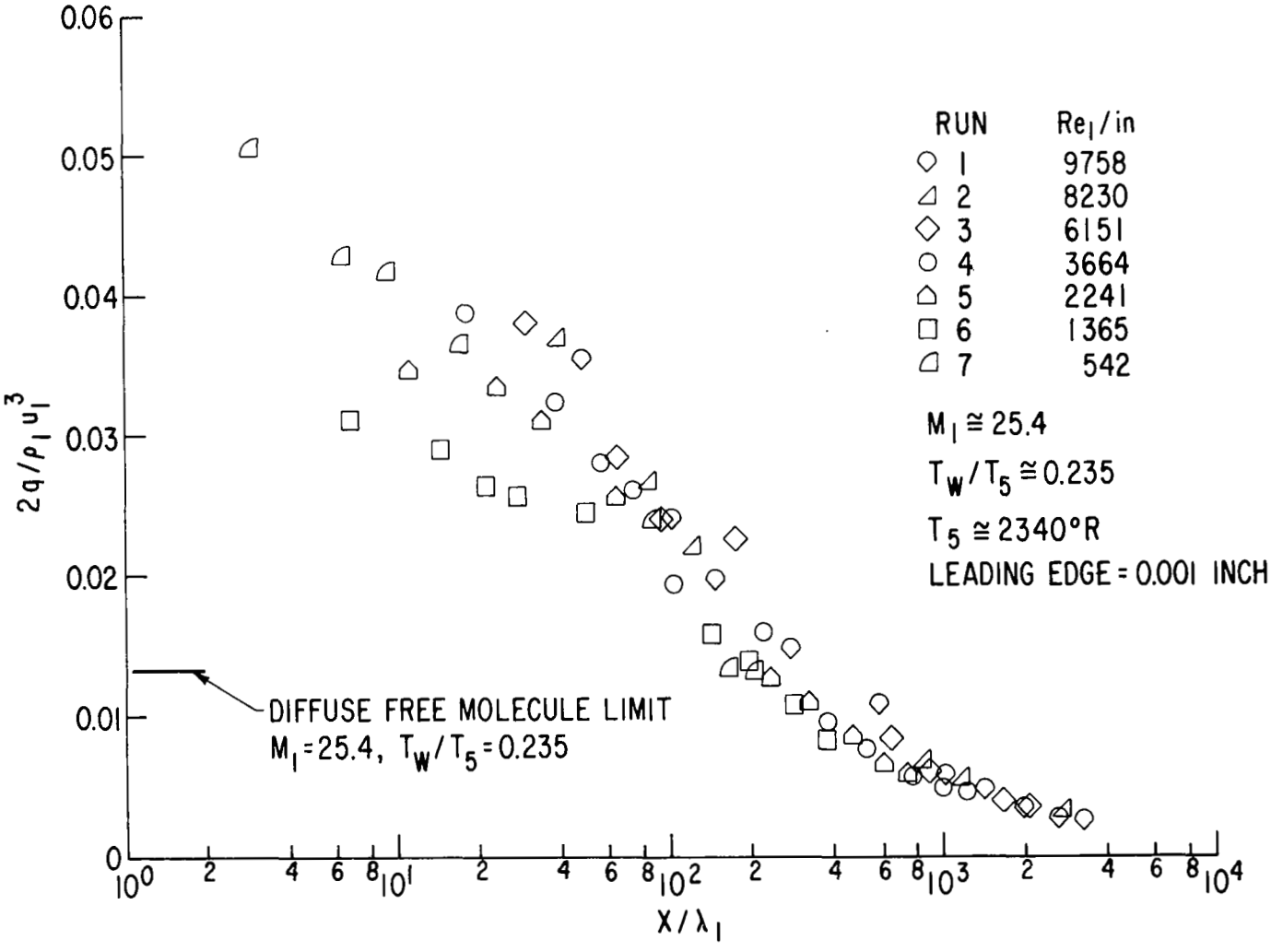

FIG. 4d NORMALIZED HEAT TRANSFER RATE vs. DISTANCE ALONG PLATE IN MEAN FREE PATHS WITH LEADING EDGE CONDITIONS, $M \cong 25.4$.

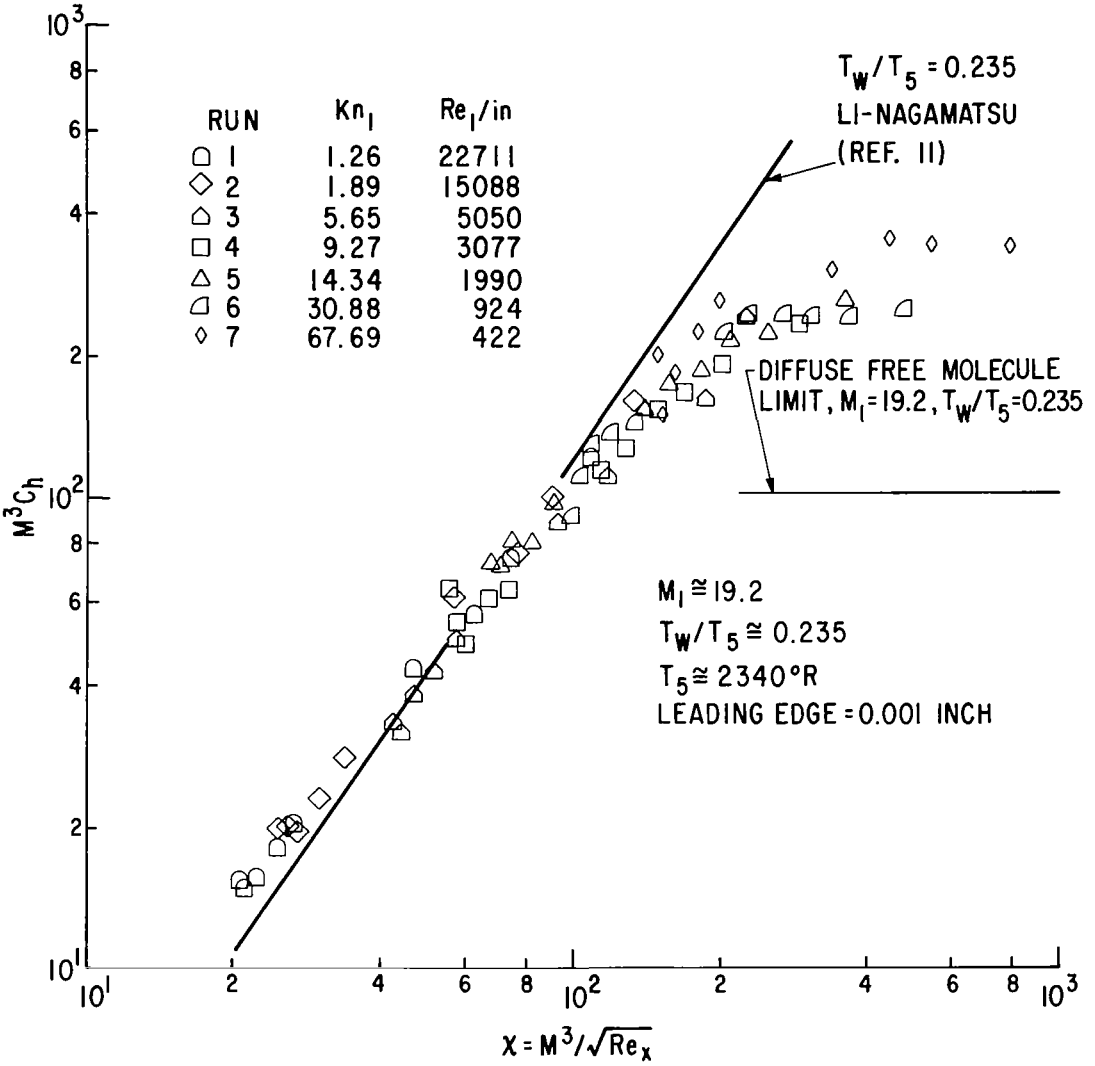

FIG.5a HEAT TRANSFER COEFFICIENT vs. STRONG INTERACTION PARAMETER WITH LOCAL CONDITIONS, M≅19.2.

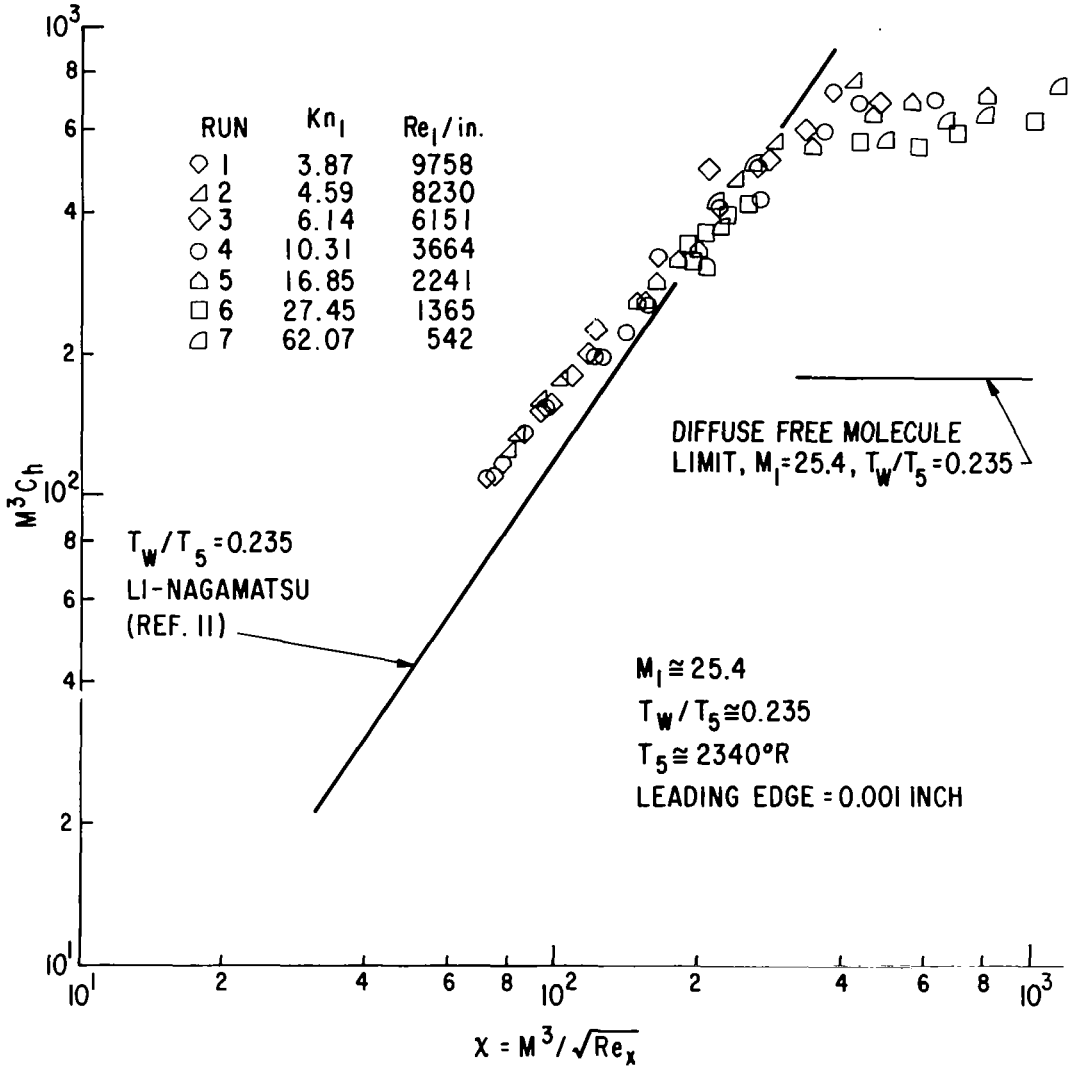

FIG.5b HEAT TRANSFER COEFFICIENT vs. STRONG INTERACTION PARAMETER WITH LOCAL CONDITIONS, M≅25.4.

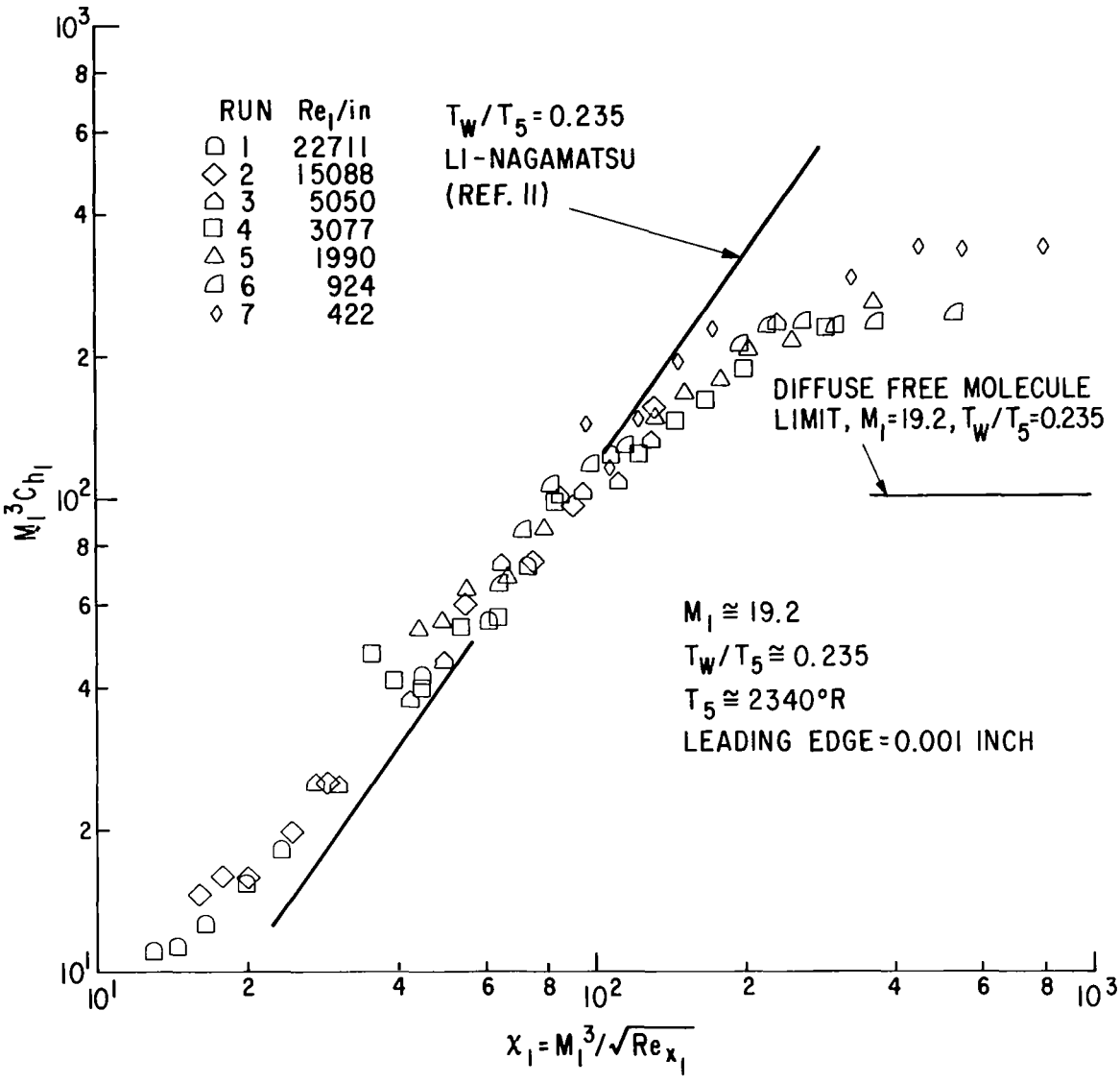

FIG.5c HEAT TRANSFER COEFFICIENT vs. STRONG INTERACTION PARAMETER WITH LEADING EDGE CONDITIONS, M ≅ 19.2.

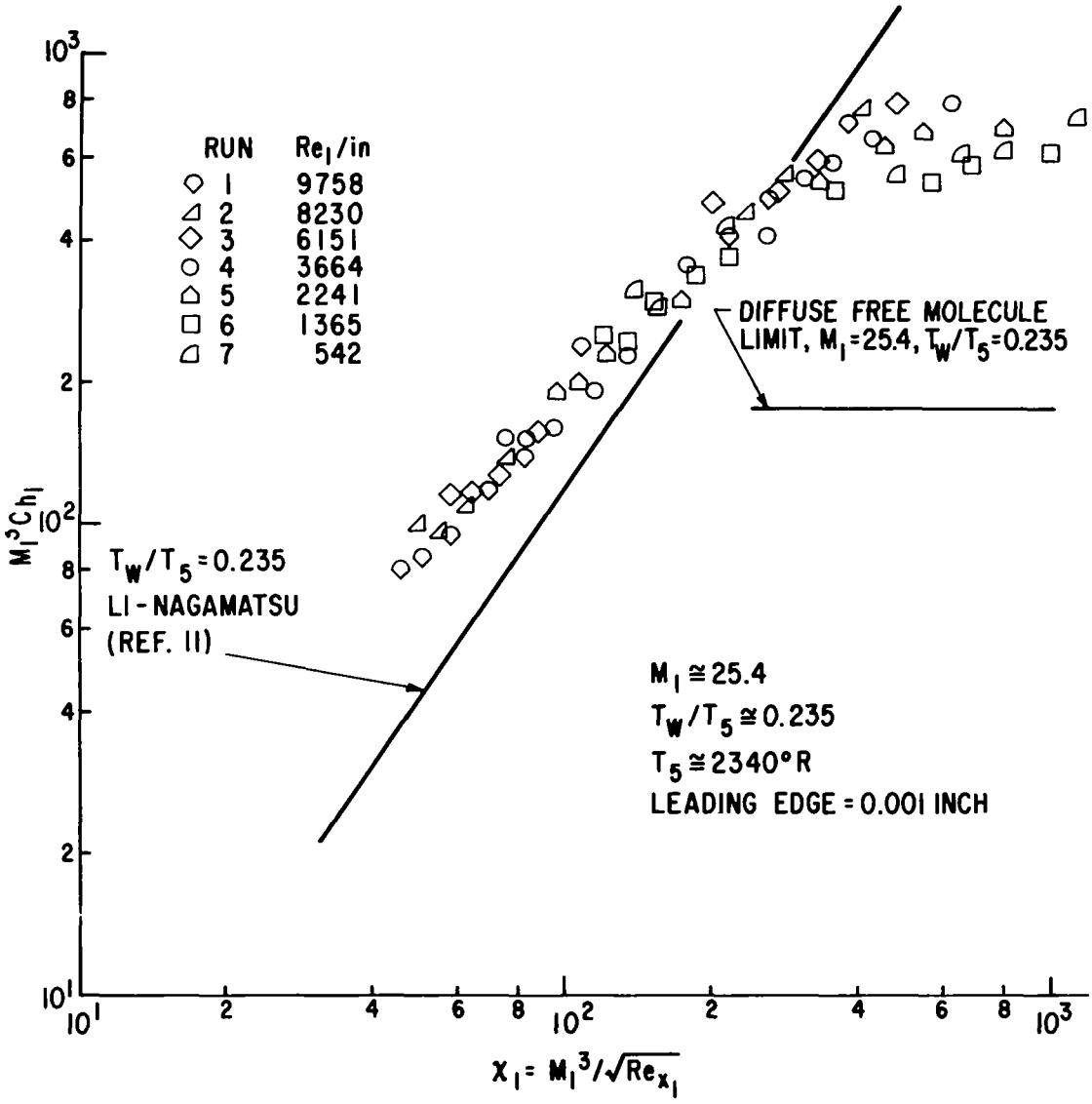

FIG.5d HEAT TRANSFER COEFFICIENT vs. STRONG INTERACTION PARAMETER WITH LEADING EDGE CONDITIONS, M≅25.4.

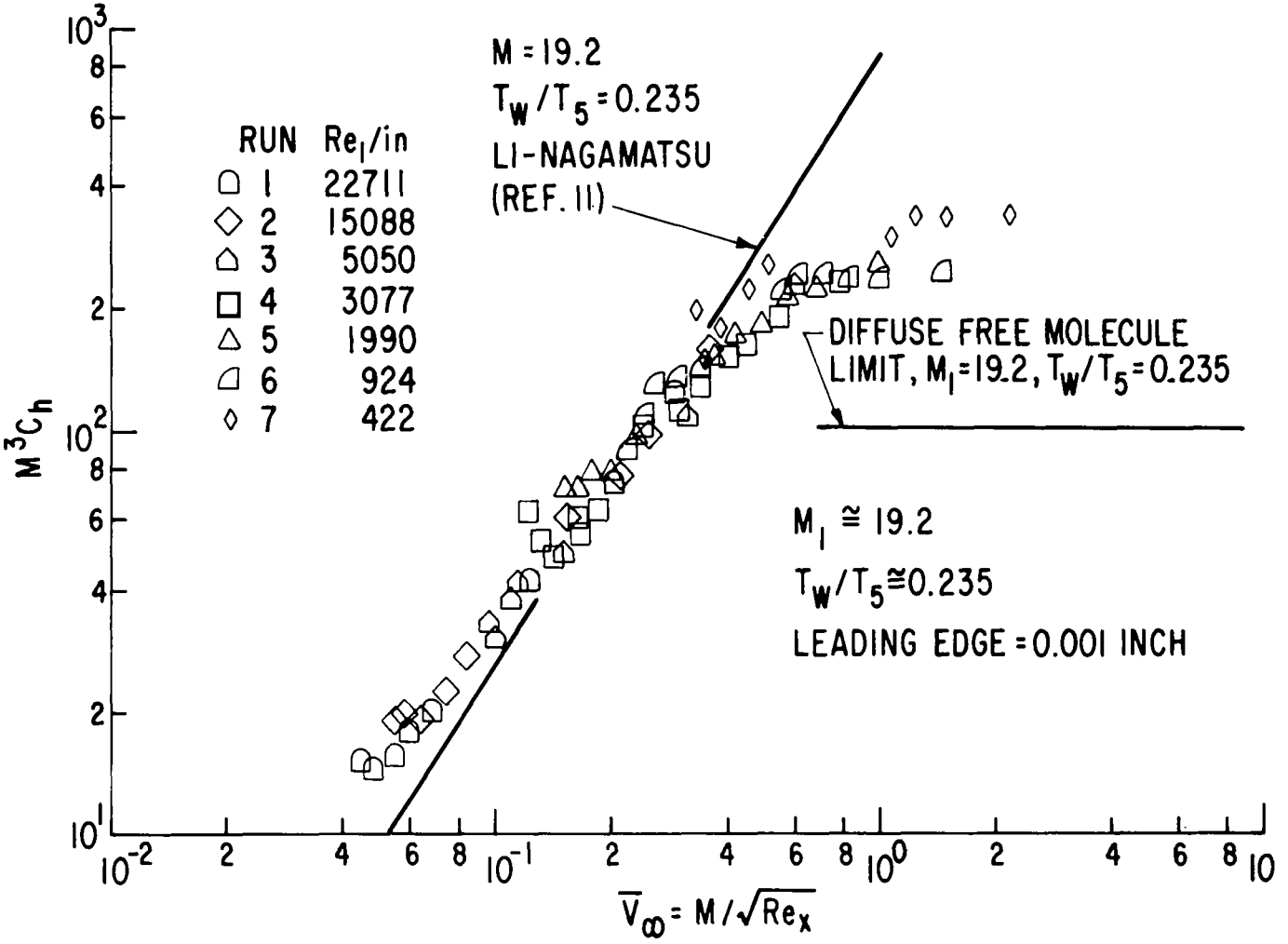

FIG.6a HEAT TRANSFER COEFFICIENT vs. RAREFACTION PARAMETER WITH LOCAL CONDITIONS, M ≅ 19.2.

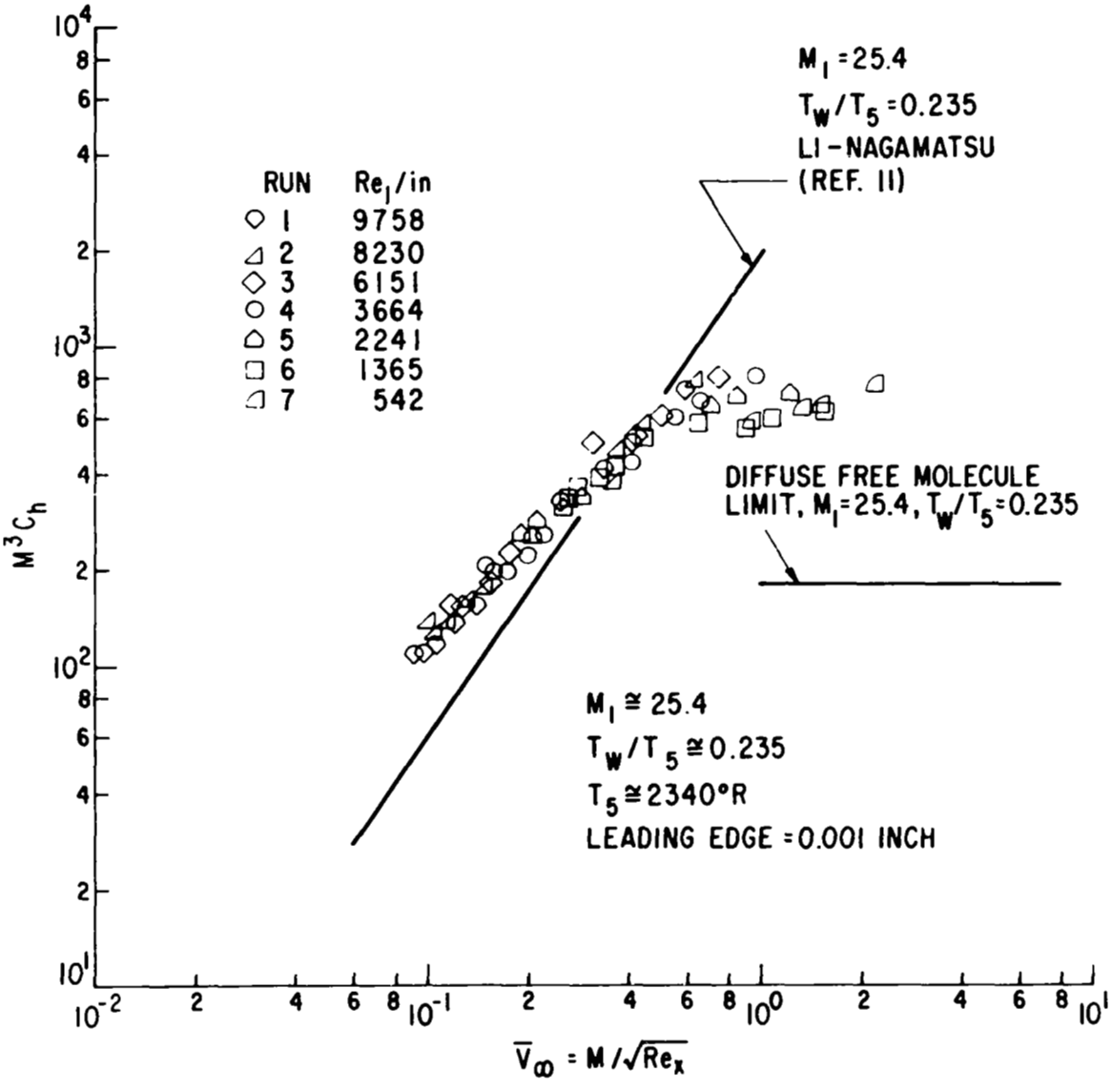

FIG. 6b HEAT TRANSFER COEFFICIENT vs. RAREFACTION PARAMETER WITH LOCAL CONDITIONS, $M \cong 25.4$.

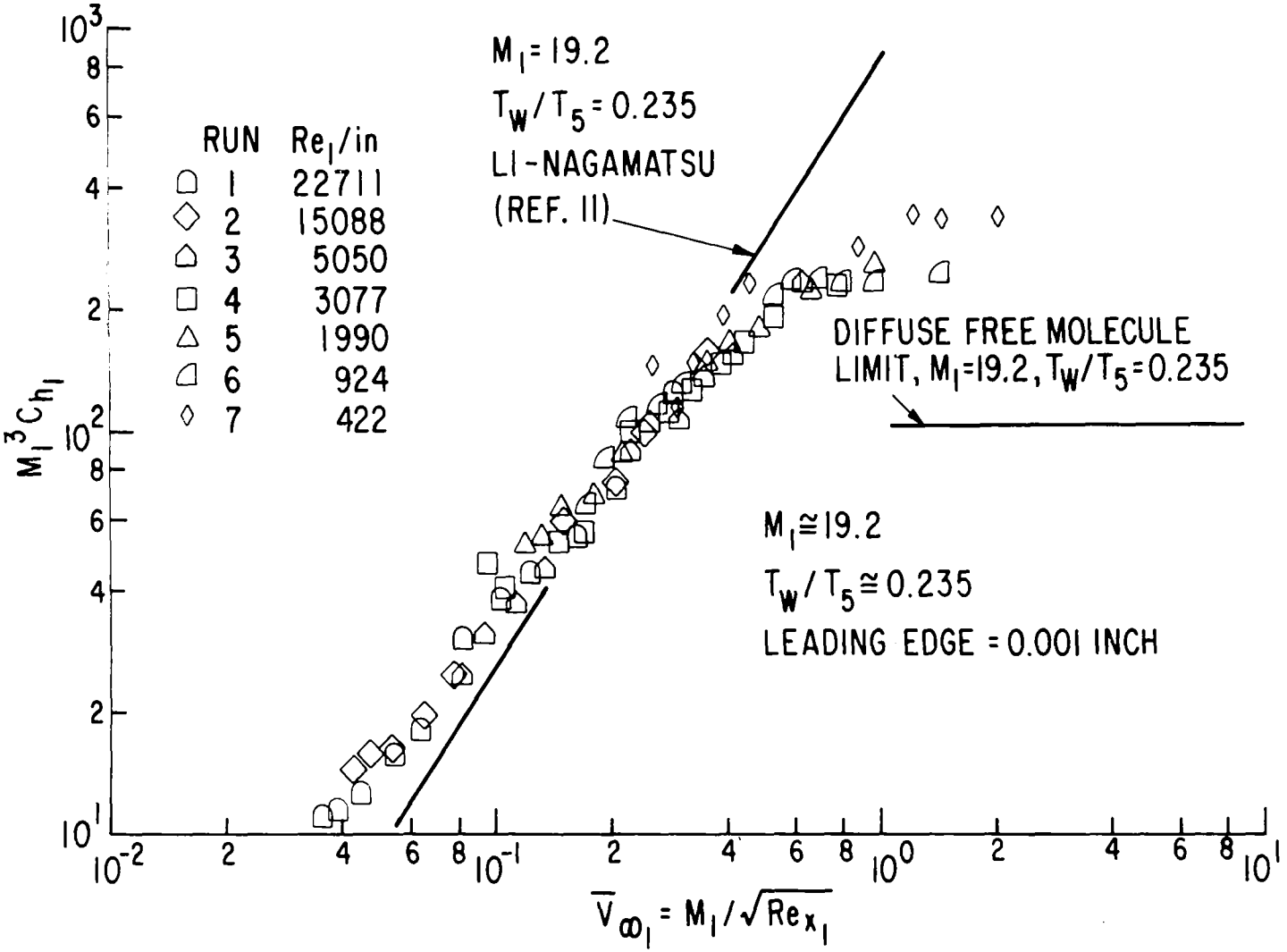

FIG. 6c HEAT TRANSFER COEFFICIENT vs. RAREFACTION PARAMETER WITH LEADING EDGE CONDITIONS, $M \cong 19.2$.

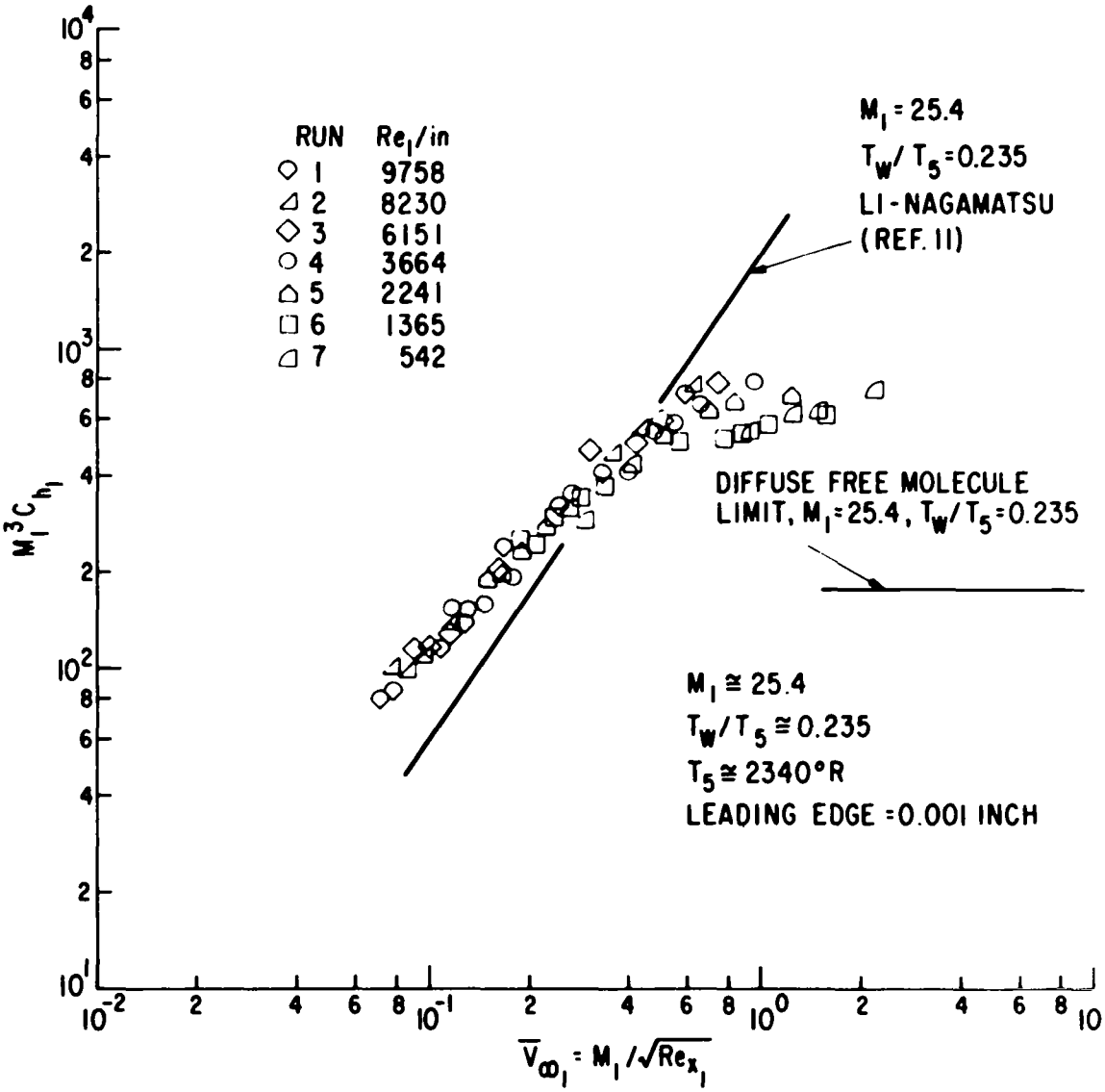

FIG. 6d HEAT TRANSFER COEFFICIENT vs. RAREFACTION PARAMETER WITH LEADING EDGE CONDITIONS, M≅25.4.

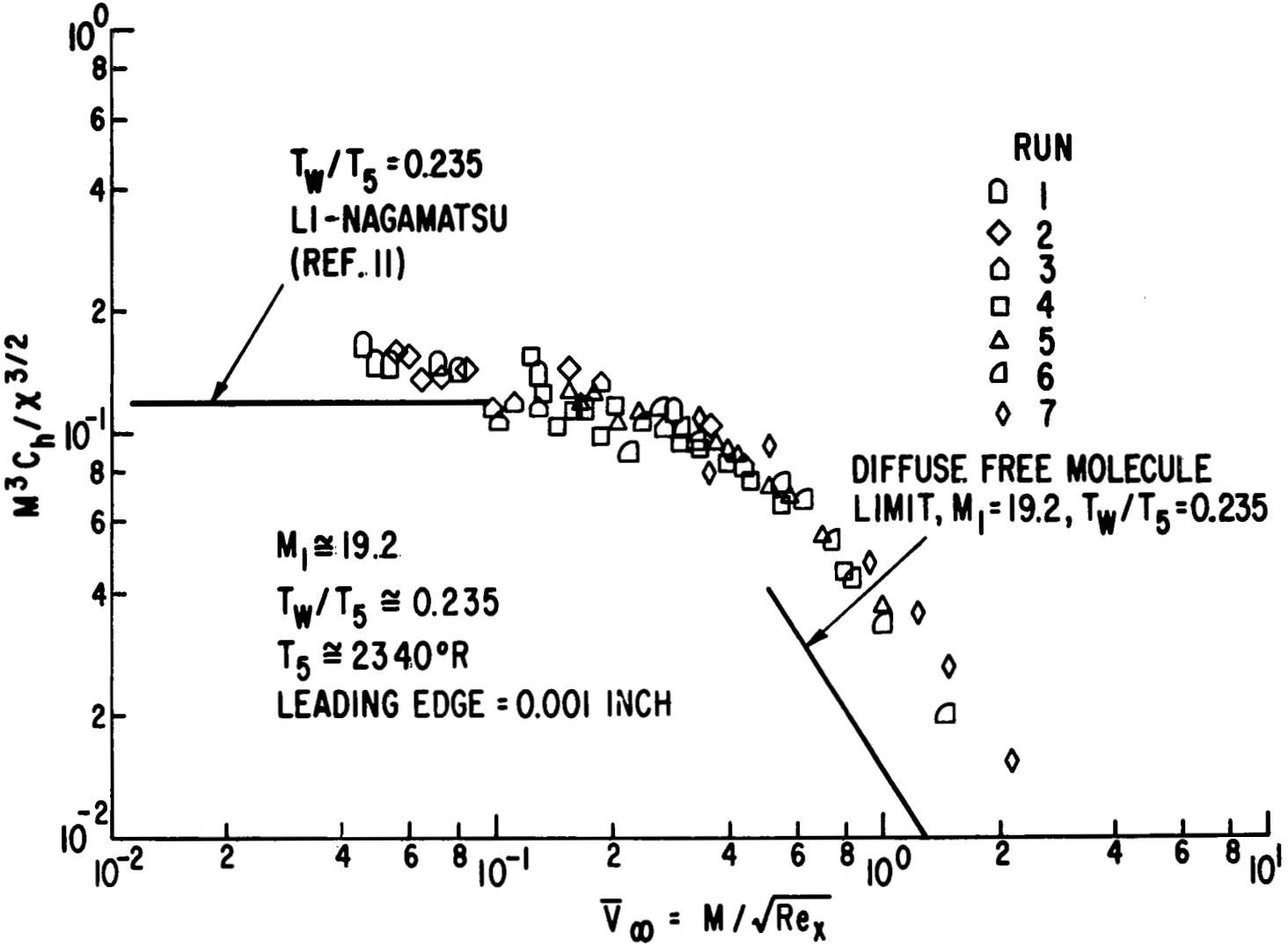

FIG. 7a NORMALIZED HEAT TRANSFER COEFFICIENT vs. RAREFACTION PARAMETER WITH LOCAL CONDITIONS, M≅19.2.

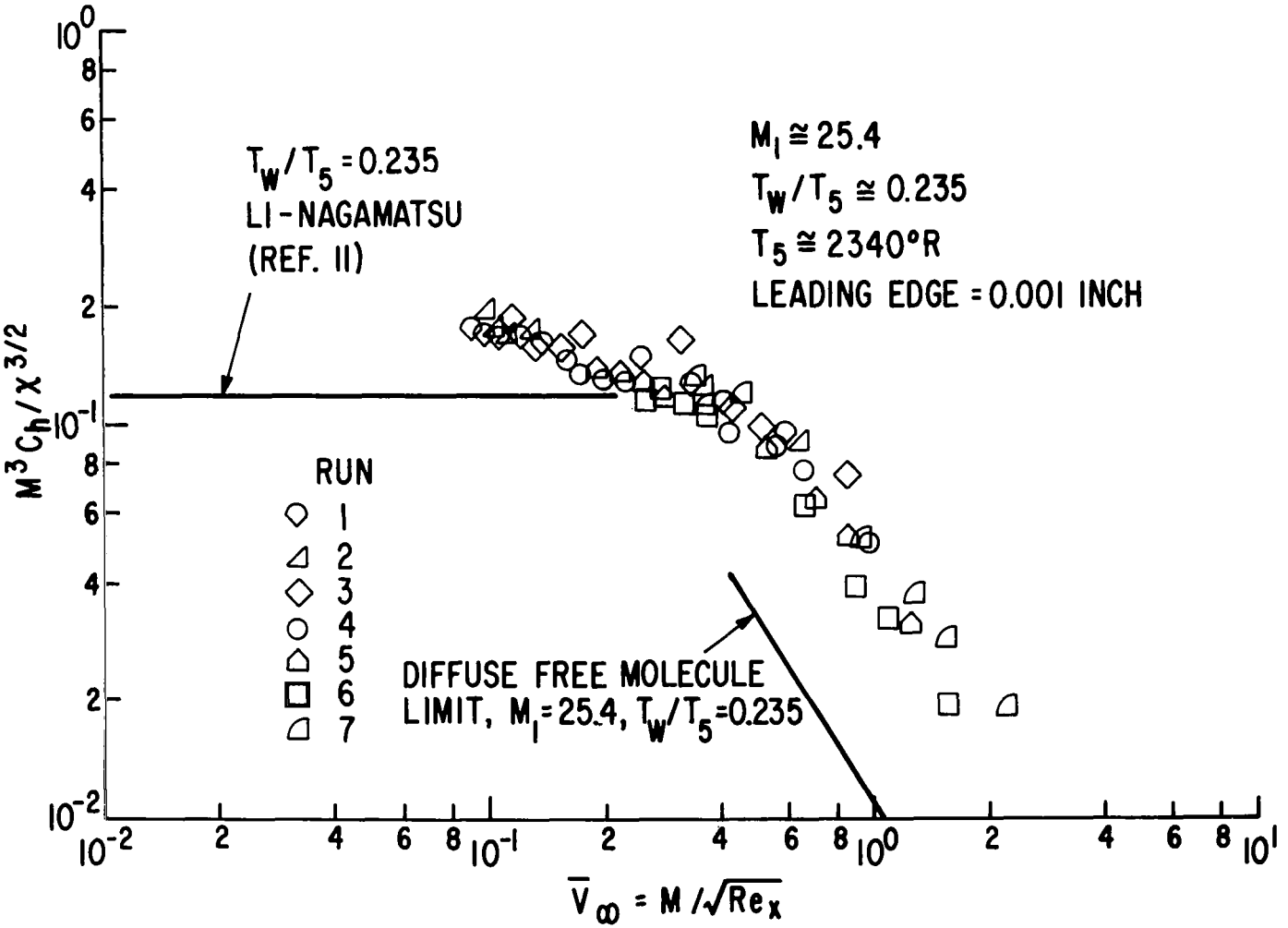

FIG. 7b NORMALIZED HEAT TRANSFER COEFFICIENT vs. RAREFACTION PARAMETER WITH LOCAL CONDITIONS, $M \cong 25.4$.

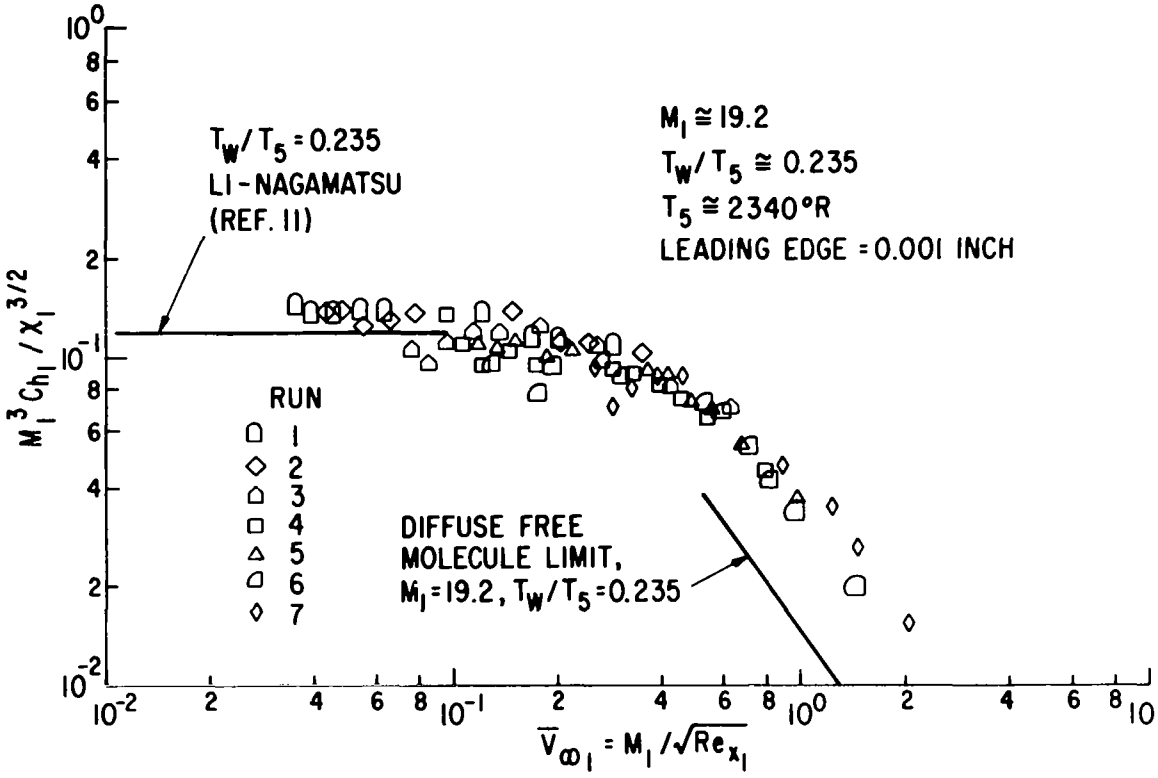

FIG. 7c NORMALIZED HEAT TRANSFER COEFFICIENT vs. RAREFACTION PARAMETER WITH LEADING EDGE CONDITIONS, M≅19.2.

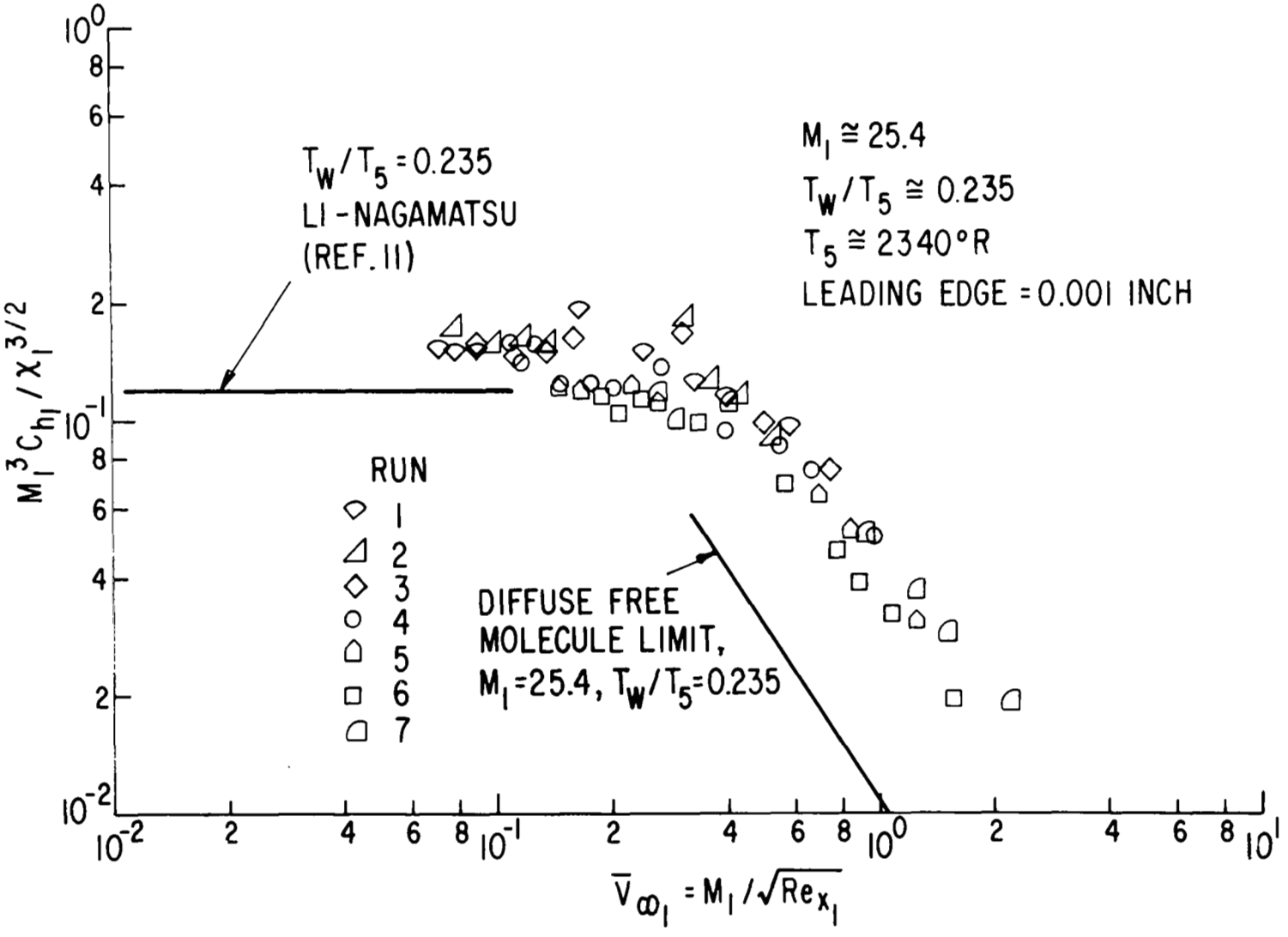

FIG. 7d NORMALIZED HEAT TRANSFER COEFFICIENT vs. RAREFACTION PARAMETER WITH LEADING EDGE CONDITIONS, M≅25.4.

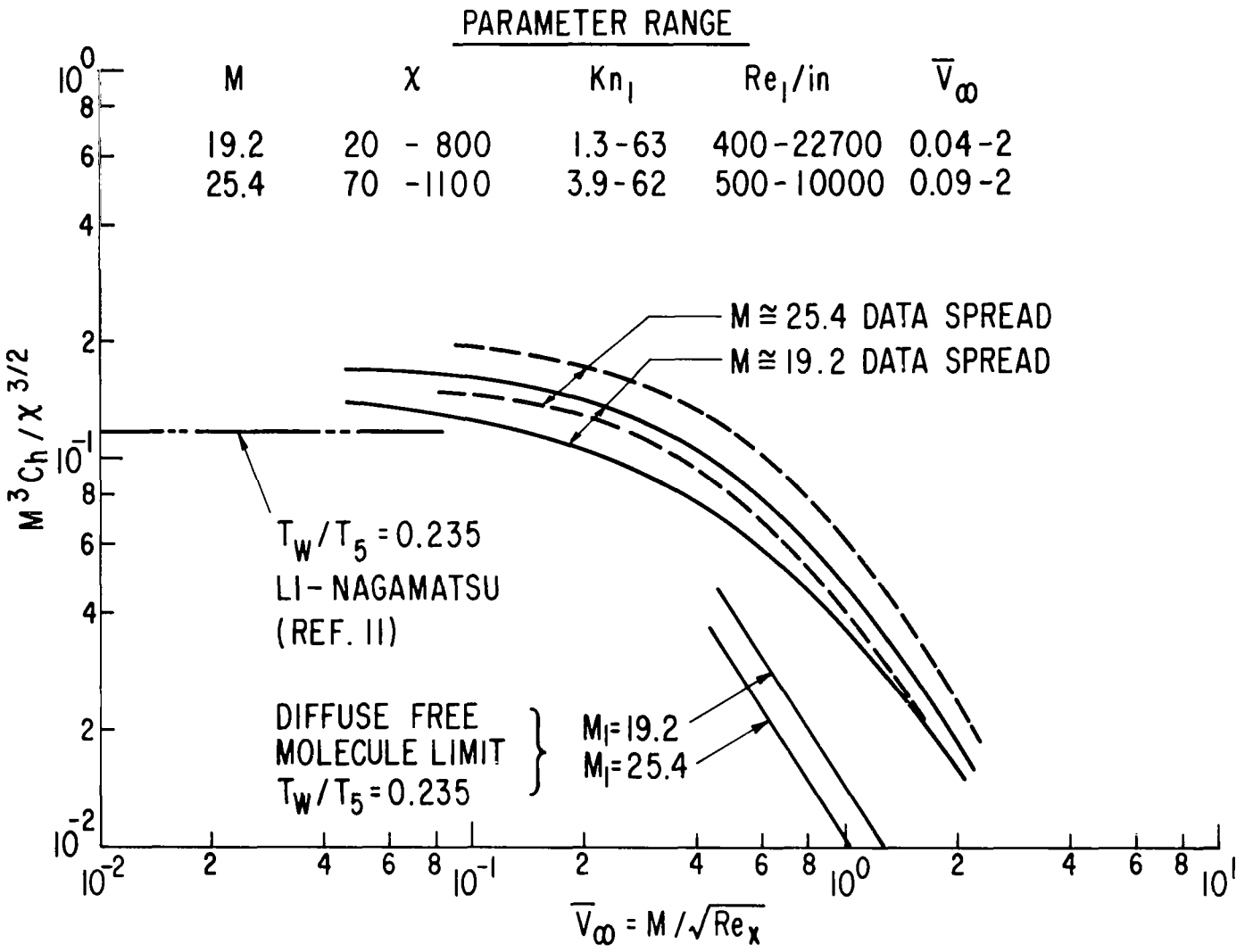

FIG. 8 CORRELATION OF M = 19 AND M = 25 HEAT TRANSFER DATA WITH LOCAL CONDITIONS, $T_5 \cong 2340°R$.

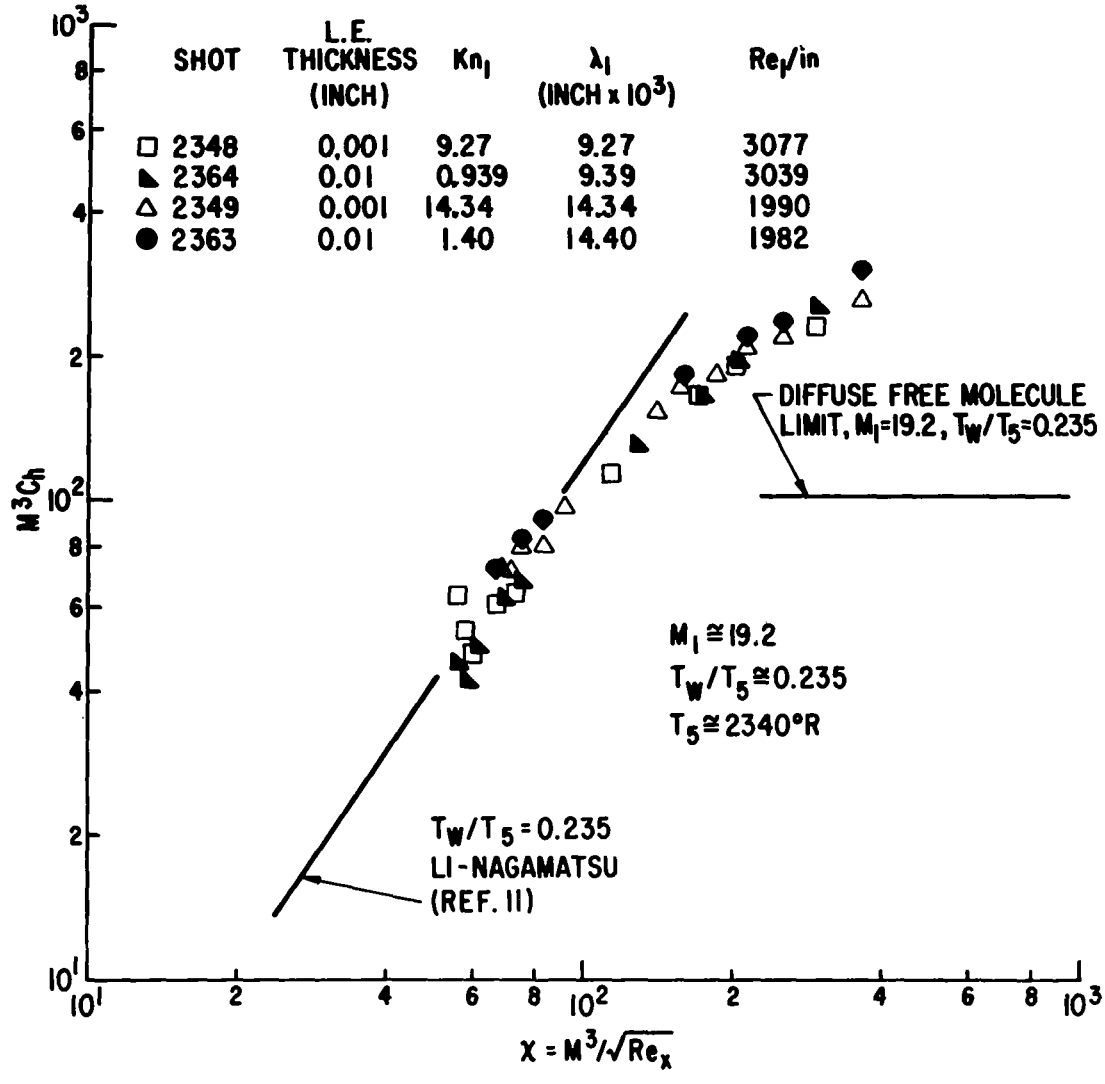

FIG. 9 EFFECT OF LEADING EDGE THICKNESS ON THE HEAT TRANSFER FOR A FLAT PLATE, M≈19.2.

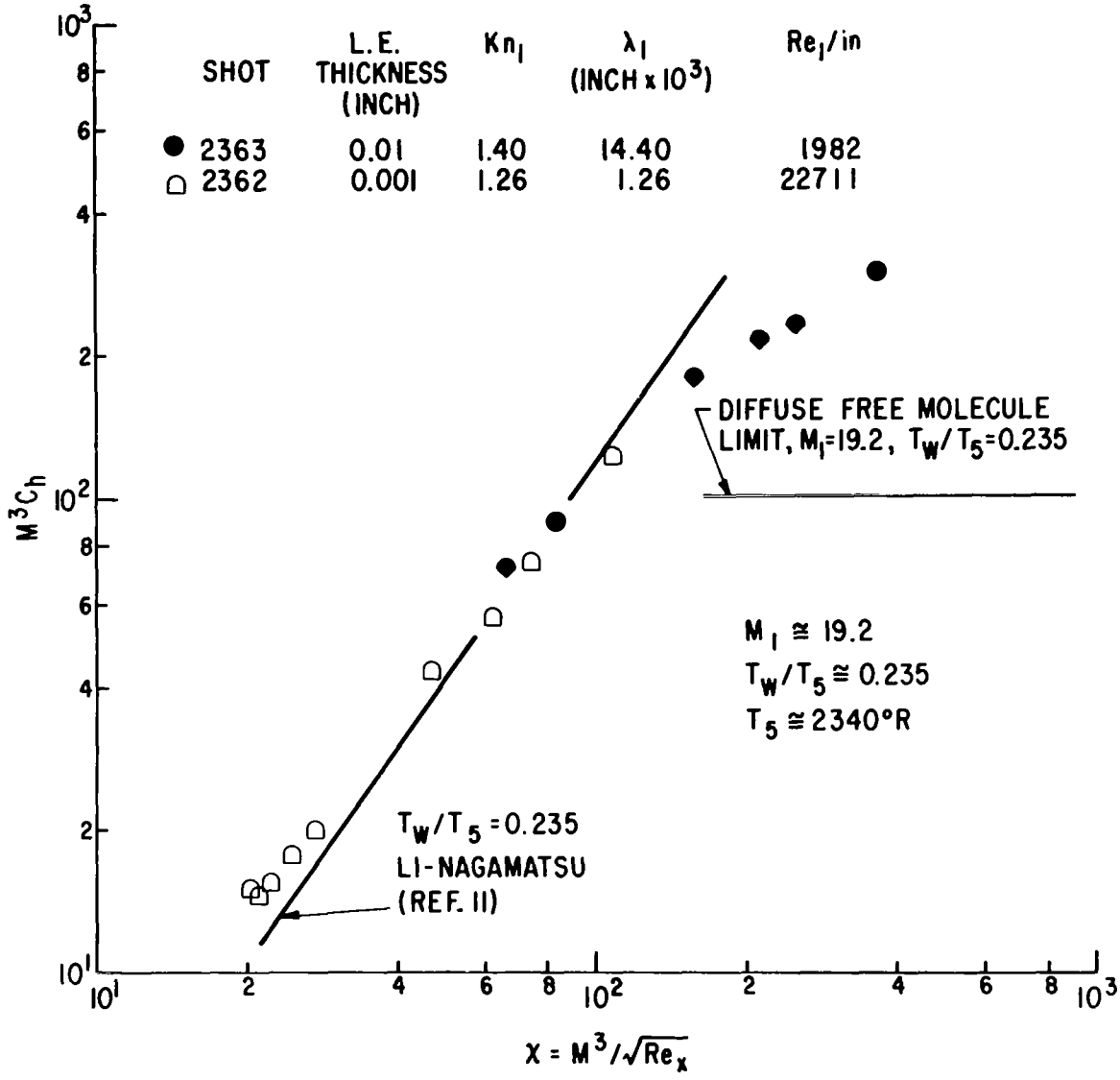

FIG. 10 EFFECT OF REYNOLDS NUMBER PER INCH ON FLAT PLATE HEAT TRANSFER, M≅19.2.

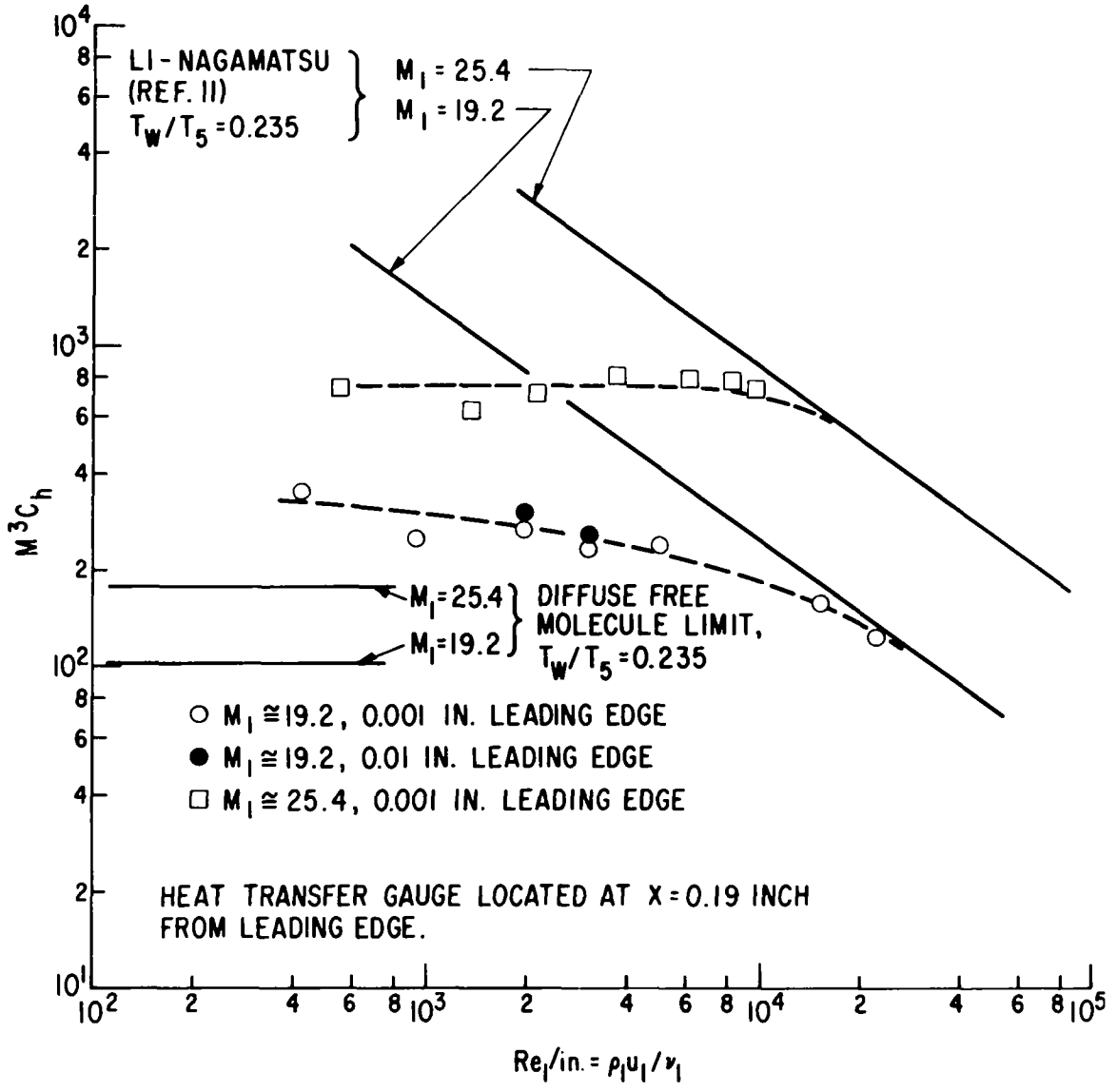

FIG. 11 EFFECT OF REYNOLDS NUMBER PER INCH ON THE HEAT TRANSFER CLOSE TO THE LEADING EDGE OF A FLAT PLATE, $T_5 \cong 2340°R$.

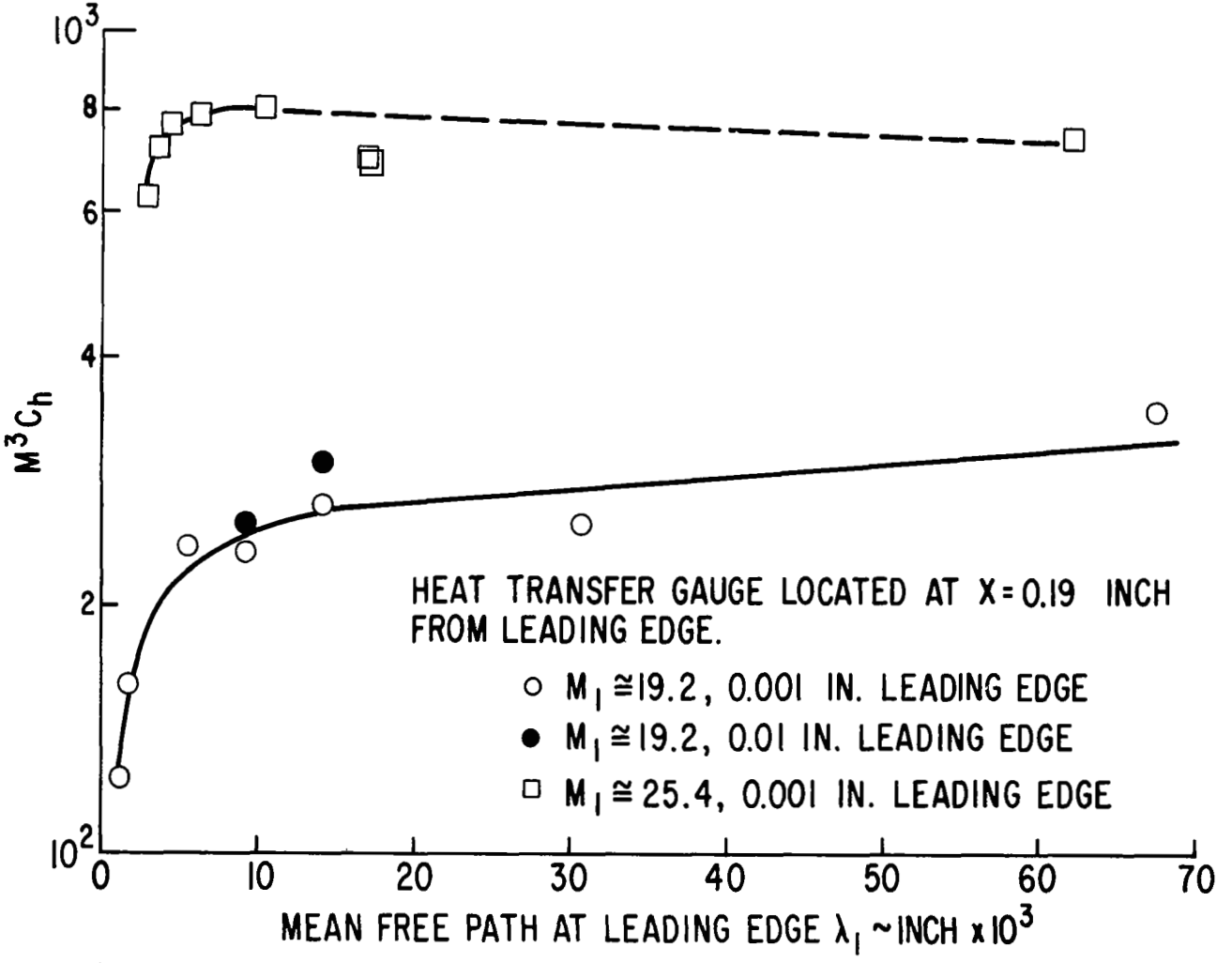

FIG.12 EFFECT OF MEAN FREE PATH ON THE HEAT TRANSFER CLOSE TO THE LEADING EDGE OF A FLAT PLATE, $T_5 \cong 2340°R$.